Response to reviewers:

#Response to Dr. Meiyun Lin

Interactive comment on "Tropospheric Ozone Seasonal and Long-term Variability as seen by lidar and surface measurements at the JPL-Table Mountain Facility, California" by M. J. Granados-Muñoz and T. Leblanc

We would like to thank Dr Meiyun Lin for her comments and suggestions. Please, find below the detailed responses.

Comments:

1. Line 80-85: The discussions on the drivers of tropospheric ozone variability are somewhat incomplete. Please consider adding a few sentences to describe the role of climate variability and associated changes in atmospheric circulation patterns in contributing to tropospheric ozone interannual variability and decadal trends, as found in the 40-year ozone record at Mauna Loa Observatory in Hawaii (Lin et al., 2014, Nature Gescience).

Meiyun Lin, L.W. Horowitz, S. J. Oltmans, A. M. Fiore, Songmiao Fan (2014): Tropospheric ozone trends at Manna Loa Observatory tied to decadal climate variability,Nature Geoscience, 7, 136-143, doi:10.1038/NGEO2066

2. In the Introduction section, you might also want to add a few overview sentences on the key role of tropopause folds on interannual variability of free tropospheric and surface ozone over the western US (e.g. Lin et al., 2015a, Nature Communications) The literature review will help in placing your Results Sections 3.2 and 3.3. into context.

Response:

The following sentences have been added to the introduction:

"Additional factors that have been observed to influence tropospheric ozone variability are climate variability and related global circulation patterns such as ENSO or PDO (e.g. Lin et al., 2014; 2015a; Neu et al., 2014). Tropopause folds also play a key role on tropospheric ozone interannual variability, as they influence the ozone budget in the troposphere and can even affect air quality near the surface (e.g. Lin et al., 2015a Brown-Steiner and Hess, 2011; Langford et al., 2012)."

Comments:

3. Line 490-493: Regarding the influence of sampling biases on calculated ozone trends, it seems like that you are discussing the results from Lin et al. (2015b, GRL). But the paper is not included in the list of references.

Meiyun Lin, L.W. Horowitz, O.R. Cooper, D. Tarasick, S. Conley, L.T. Iraci, B. Johnson, T. Leblanc, I. Petropavlovskikh, E.L. Yates (2015): Revisiting the evidence of increasing

springtime ozone mixing ratios in the free troposphere over western North America, Geophysical Research Letter, 42, doi:10.1002/2015GL065311

Response:

The paper was missing from the reference list. It is now included.

Comment:
4. Line 500-503: Discussions here are somewhat awkward. Are you talking about long-term trends or seasonal variability? I don't believe anyone has suggested that the negative trends (if any) in wintertime ozone over the western US are due to a decrease in background ozone.

Response:
Discussion refers to long term trends. Negative trends were observed at some stations in Cooper et al., (2012) during wintertime, even though most of them were not significant. A significant negative trend is also observed for the median values in this study from 4 up to 10 km during wintertime. The comment on the background ozone decrease has been removed considering all the comments in this respect.

Comment:
5. Line 510: None of the cited references has explicitly discussed the influence from stratospheric intrusions. You should cite other more relevant papers.

Response:
The studies by Cooper et al., 2010 and Parrish et al., 2009, provide information about the different regional behavior observed between the western and the eastern US regarding ozone trends. These studies explain the causes for this difference, including both the Asian transport and stratospheric influence affecting predominantly the Western region. References Lin et al., (2012a; 2015a) and Lefohn et al., (2011; 2012) have been included for completeness.

#Response to Reviewer 1

Interactive comment on "Tropospheric Ozone Seasonal and Long-term Variability as seen by lidar and surface measurements at the JPL-Table Mountain Facility, California" by M. J. Granados-Muñoz and T. Leblanc

Anonymous Referee #1

Received and published: 13 April 2016

MS Number: acp-2016-70

Summary:

This paper by Maria Jose Granados-Munoz and Thierry Leblanc presents an interesting analysis of tropospheric ozone profiles over the JPL-Table Mountain Facility, California, based on 16 years of regular Lidar measurements and 2 years of co-located surface measurements. The manuscript spans different aspects of what such an extensive data set allows in terms of characteristics of ozone vertical distribution: diurnal and seasonal cycles, vertical variability from 2 to 20 km, interannual variability and trends between 2000 and 2015, classification of air mass origins, and influence of tropopause folds.

Authors are right, such extensive ozone data set from JPL-TMF is "very valuable due to the rising interest in the detection of long-term trends in the Western United States : : :" as written in the introduction. Such extensive tropospheric ozone data set has not been presented in publication before and thus deserves a reference paper. The title, as well as the last sentences of the introduction are promising and gives expectations on the understanding of the observed long-term variability. However, the manuscript misses some diagnostics and solid conclusions to provide a thorough assessment to be used by a broad audience. It seems that the manuscript is a compilation of independent sub-sections and the primary objective of understanding the long-term vertical variability has been lost at the end. Subsection 3.5 in particular does not help at all in understanding the interannual variability. Similar remark applies for sub-section 3.4, which is also leading to unexpected conclusion on "No outstanding influence from Asia" as highlighted in the abstract. As a consequence, the discussion and concluding remarks sections do not appear robust enough at this stage of the manuscript. They are sometimes in contradiction with previous findings and let the reader with a promise of a following paper after additional analysis is performed. It's unfortunate.

Regarding the presentation of the manuscript, it is also not very comfortable to have to wait the discussion section to read conclusions and explanation on what have been observed and described in previous sub-sections. I would strongly recommend to include the different paragraphs of the section 4 in their associated sub-sections 3. Undoubtedly, this

manuscript is meant to be a valuable contribution, especially because it is an impressive long-term data set but I have major concerns regarding the robustness of some analysis and conclusions. Therefore, I will recommend publication only after (major and minor) revisions as detailed below are considered. Finally, I support what M.-Y. Lin has posted as an interactive comment and recommend the authors to also follow her recommendations.

Response:

First of all, we would like to thank the reviewer for the comments and suggestions which have helped to improve the quality of the manuscript. Especially, section 3.4 is now much improved and more significant results were found. Comments and suggestions have been really helpful to improve the section and the quality of the manuscript.

The study presents the tropospheric ozone lidar database acquired at TMF, which has not been previously presented in a peer reviewed publication and we consider it is of high interest due to its characteristics. As the reviewer says, the data set allows characterizing the diurnal and seasonal cycles, vertical variability, interannual variability and trends and the influence of different sources affecting the ozone profiles measured at the station. Sections 3.4 and 3.5 are mainly intended to contribute to the characterization of tropospheric ozone above TMF and to analyze the influence of the different sources on the ozone profiles. However, the goal of using them to understand the long-term variability is too ambitious for this study. Trends related to the different air masses categories presented in Section 3.4 and trends in the tropopause folds and their possible influence on the interannual variability has been investigated, but no statistically significant results were observed because the number of data is drastically reduced when subdivided in smaller datasets. Nonetheless, we think this analysis deserves an additional publication where the lidar database is combined with additional data (e.g. model, satellite, additional stations…) to reach significant results and conclusions in this respect.

Regarding the influence from Asia, section 3.4 has been rewritten based on the new criteria used for the classification of the air masses (see following responses).

Discussion section has now been suppressed and the comments are included in the corresponding subsections of the results as suggested by the reviewer. Recommendations and comments by Meiyun Lin have also been addressed.

Major comments:
-Abstract, line 53: This last sentence "No outstanding influence from Asia was identified" is quite surprising, in contradiction with previous studies, and raises issues on the robustness of the methodology. See further comments below.

Response:
The abstract has been modified according to the new results obtained in Section 3.4. The sentence is no longer included. Instead, the following sentence has been added:

Lines 55-56: *"Influence from Asia was observed throughout the year, with more frequent episodes during spring, associated to ozone values from 53 to 63 ppbv at 9 km."*

- Line 99: The characteristic "only surface or column-integrated measurements" does not apply to aircraft (MOZAIC/IAGOS) platforms. Zbinden et al., (2013) give a recent detailed description of ozone vertical profiles by MOZAIC/IAGOS over mostly documented airports by the program since 1995 (including Los Angeles airport). Logan et al., (2012) also used vertical profiles recorded by MOZAIC aircraft in addition to ozone sondes for deriving a global picture of ozone trends over Europe.

Response:
Information regarding aircraft platforms and the suggested references have been included in the introduction.
Lines 114-117: *"Ozone vertical profiles have also been obtained from aircraft platforms through programs such as MOZAIC and IAGOS, available since 1995 (e.g. Zbinden et al., 2013, Logan et al., 2012). However, aircraft data are limited to air traffic routes and the temporal resolution depends on the frequency of the commercial flights."*

Comment:
- Lines 167 to 177: This paragraph as well as associated Figure 1 are questionable. It seems surprising to see on figure 1a that the difference is not varying with altitude. Given the argument from the last sentence of the paragraph that sampled air masses are not the same, one could expect a higher difference in regions with higher ozone variability (UTLS compared to free troposphere). It is not the case. Concluding the section with differences within +/- 15% raises the question on the regional representativeness of the JPL-TMF station. This paragraph deserves much more attention and details to give proof on the consistency between those two independent data sets (if that was the objective of such paragraph ?).

Response:

The objective of the paragraph is to show the accuracy of the lidar measurements using for validation an independent and reliable technique such as the ECC, since lidar measurements from the DIAL at JPL-TMF have not been presented before. The paragraph has been modified and additional details are now provided.
The effect of the drift of the ozonesonde is not visible in figure 1 due to the larger ozone values observed in the UTLS region compared to the troposphere. We see an increase in the difference when we represent the RMSE (see figure below), but the relative differences expressed in percentage remain almost constant with altitude.
The average difference between the lidar data and the ECC (7% in the troposphere) is within the ranges observed in previous studies (see e.g. Sullivan et al., 2015) for lidar systems and it is a reasonable value considering the differences between both techniques. The 15 % value has been replaced by 10%, which is more accurate in view of the plots in figure 1 and the paragraph has been rewritten.

Lines 180-194: *"The TMF ozone lidar measurements have been regularly validated using simultaneous and co-located Electrochemical Concentration Cell (ECC) sonde measurements (Komhyr, 1969; Smit et al., 2007). In the troposphere the precision of the ozonesonde measurement is approximately 3-5% with accuracy of 5-10% below 30 km. TMF has ozonesonde launch capability since 2005 and 32 coincident profiles were obtained over the period 2005-2013. Results from the lidar and the ECC comparison are included in Figure 1.Figure1a shows the averaged relative difference between the lidar and ECC ozone number density profiles for the 32 cases. On average, the lidar and sonde measurements are found to be in good agreement, with an average difference of 7% in the bulk of the troposphere and most of the values under 10% (Figure 1b), which is within the combined uncertainty computed from both the lidar and sonde measurements. Note that a non-negligible fraction of the differences is due to the different measurement geometry of the lidar and ozonesonde: 2-hour averaged, single location for lidar, and horizontally-drifting 1-second measurements for the ozonesonde usually rising at 5 $m \cdot s^{-1}$. Figure 1c reveals that the deviations do not present significant changes with time, which is an indicator of the system stability despite the multiple upgrades made over this time period."*

Reference:

Sullivan, John T., Thomas J. McGee, Russell DeYoung, Laurence W. Twigg, Grant K. Sumnicht, Denis Pliutau, Travis Knepp, and William Carrion. "Results from the NASA GSFC and LaRC ozone lidar intercomparison: New mobile tools for atmospheric research." Journal of Atmospheric and Oceanic Technology 32, no. 10, 1779-1795, 2015.

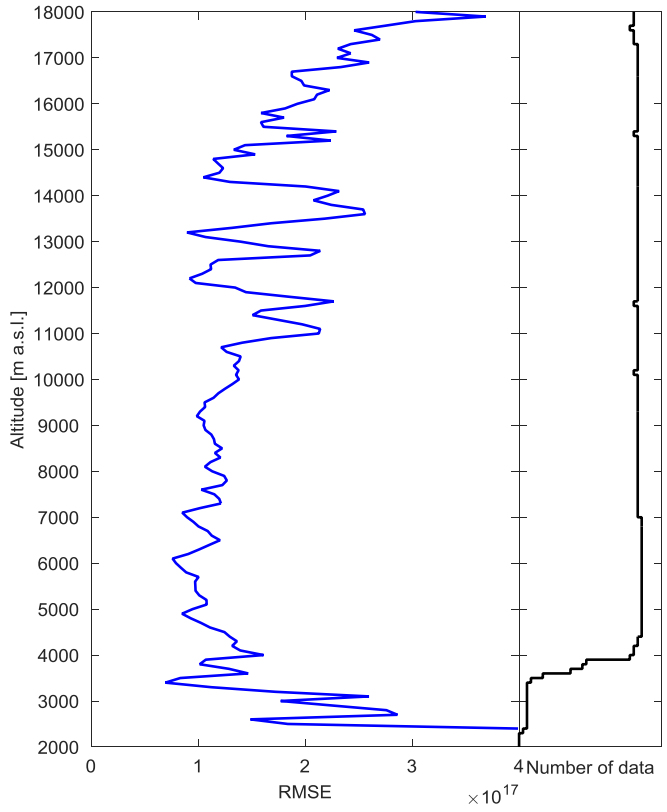

Figure. a) Profile of RMSE for the lidar compared to the ECC ozone number density for the 32 simultaneous measurements (dark blue). The black solid curve shows the number of data points at each altitude.

Comment:
- Line 184: This paragraph omits to give appropriate accuracy/error procedures of this analyzer and reference (at least from previous use of such type of instrument). Information on operating procedures (maintenance, calibration), or at least a reference paper would be appreciated.

Response:
References has been included and some additional information about uncertainty. Calibration was performed after the installation of the instrument at JPL-TMF and will be recalibrated during next summer.

Lines 196-203: *"Continuous surface ozone measurements have been performed at TMF since 2013 using the UV photometry technique (Huntzicker et al., 1979) with a UV photometric ozone analyzer (Model 49i from Thermo Fisher Scientific, US). The operation principle is based on the absorption of UV light at 254 nm by the ozone molecules (Shina et al., 2014). The instrument collects in-situ air samples at 2 meter above ground taken from an undisturbed forested environment adjacent to the lidar building. It provides ozone mixing ratio values at 1-minute time intervals with a lower detection limit of 1 ppbv. Uncertainty has been reported to be below 6% in previous studies (Shina et al., 2014)"*

Comment:
- Line 241: Figure 3a is not restricted to the tropospheric part of the ozone profile. Either change this adjective in the sentence or the figure. The title of the paper and of the sub-section is clearly on tropospheric ozone variability. I suggest to plot Figure 3 only for altitudes up to 15 km (on average) and modify the X axis for linear concentrations on the tropospheric typical range [0-150 ppb]. In the seasonal part of the Figure 3, that will give the advantage to further see differences between the averaged seasonal vertical profiles. Is the spring profile that close to the summer profile ? From Figure 4, it seems that the spring profile should highlight higher ozone that the summer one.

Response:
The paper is mainly focused on the tropospheric region. Nonetheless, ozone information in the UTLS region is very valuable and affects the ozone budget in the troposphere. Therefore we consider this information is relevant and should be maintained in the study. The sentence has been modified accordingly. A zoomed version of figure 3 has been included also in the manuscript to see more clearly the seasonal differences in the tropospheric part of the profiles. Larger values are observed in spring, but differences with summer are not very large.

Comment:
- Lines 268-270: The spring-summer maximum is indeed a common characteristic of northern mid-latitudes over Europe and North-America. However, it seems that these JPL-TMF data as shown in Figure 4 shows a clear spring maximum (at least April-May). This

seems actually consistent with what Zbinden et al, (2013) have shown over Los Angeles airport based on MOZAIC data. This paragraph deserves further clarification to highlight this "local" characteristic of a clear spring maximum (if confirmed by Figure 3 plotted with a tropospheric X axis only). This special feature is likely the result of stronger influence from Asia in spring over the west coast of the US (Jaffe et al.2003; Parrish et al., 2004; Cooper et al., 2005; Neuman et al., 2012) as mentioned by Zbinden et al., (2013). Therefore, it is very surprising to read in the abstract that "No outstanding influence from Asia was identified". I am not convinced by such statement. Further comments below regarding subsection 3.4.

Response:

In the paper by Zbinden et al., (2013) a strong maximum is observed in spring whereas values in summer are close to those observed in fall. At JPL-TMF, there is a maximum in spring but values are very similar to those observed in summer and clearly distinct from those in fall and winter (see attached figure and new version of Figure 3). Discrepancies between both datasets can be easily explained considering the different sampling periods (1994-2009 in Zbinden et al., (2013)) and the lower number of profiles (300 and <42 monthly profiles) used in the study by Zbinden et al., (2013).

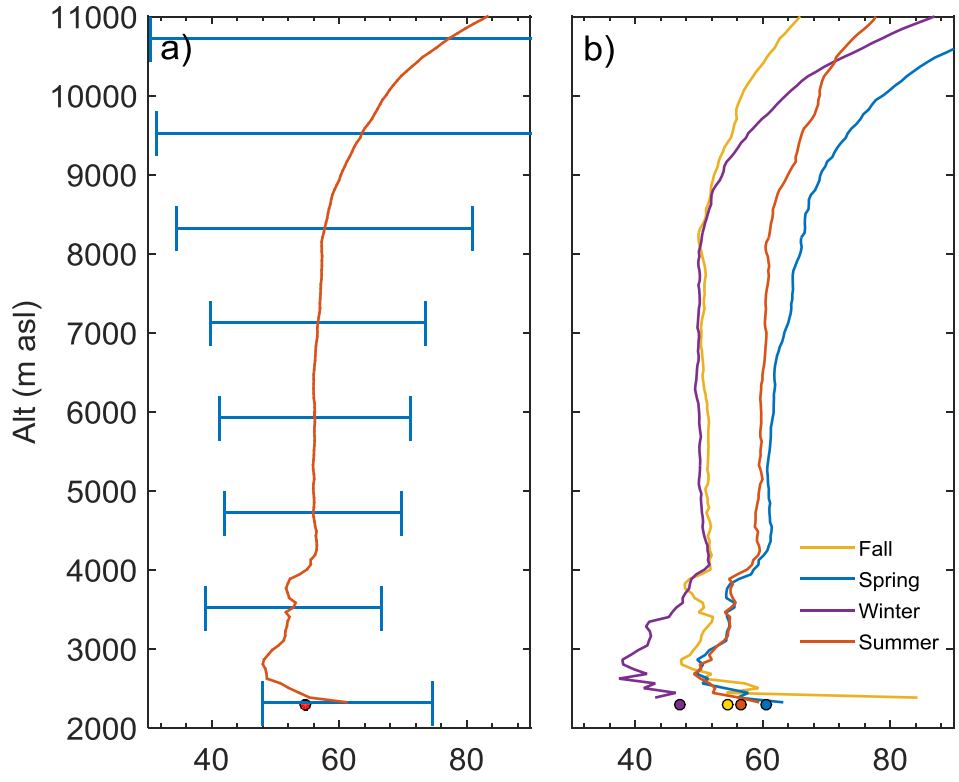

Figure. a) Ozone mixing ratio climatological average (2000-2015) computed from the TMF lidar measurements (red curve). The cyan horizontal bars indicate the standard deviation at intervals of 1-km. The red dot at the bottom indicates the mean surface ozone mixing ratio (2013-2015) measured simultaneously with lidar. b) Seasonally-averaged ozone mixing ratio profiles for spring (MAM), summer (JJA), fall (SON) and winter (DJF).

Comment:
- Lines 302-311: As far as I know, the common rule for indicator of the statistical significance of the trends with such procedure is to use p-Values lower than 0.05 for trends with a confidence level larger than 95% (and not p larger than 0.1 and confidence level larger than 90%). I recommend the authors to rewrite tables 2 and 3 applying these criteria. It turns out that only spring (in the upper troposphere) and winter (from 4 to 10 km) show significant seasonal trends. It would also be nice to give indication of error in % in first part of Table 3 as done in Table 2.

Response:
A discussion using p-Values of 0.05 is also included to ease comparison with previous studies. Nonetheless, the criterion of p-Values lower than 0.1 is used in atmospheric sciences (e. g. Xia et al., 2008; Wilson et al., 2012) and we consider it is worthy to maintain it in the study. A confidence level larger than 90% is still quite significant and these trends should not be neglected. Tables and text has been modified accordingly. Error in % is now included in Table 3 as suggested by the reviewer.

Xia, X., T. F. Eck, B. N. Holben, G. Phillippe, and H. Chen (2008), Analysis of the weekly cycle of aerosol optical depth using AERONET and MODIS data, J. Geophys. Res., 113, D14217, doi:10.1029/2007JD009604.

Wilson, R. C., Fleming, Z. L., Monks, P. S., Clain, G., Henne, S., Konovalov, I. B., Szopa, S., and Menut, L.: Have primary emission reduction measures reduced ozone across Europe? An analysis of European rural background ozone trends 1996–2005, Atmos. Chem. Phys., 12, 437-454, doi:10.5194/acp-12-437-2012, 2012.

Comment:
- Lines 322-328: This decrease in winter is the most surprising information of this paper. As far as I know, there is no other reference mentioning such significant decrease in winter in the region. In the recent review paper of Cooper et al., 2014 (and references therein including Cooper et al., (2012)), reported stations in California do show significant increase in winter. Therefore I recommend the authors to further argue and explain why such a different behavior at JPL-TMF station. This entire subsection misses further discussion on this trends analysis. See additional comments below regarding section 4.

Response:
As previously stated, the analysis on the causes of the different trends is not straightforward and it is worthy an additional paper using complementary data (i.e. model, satellite, sounding data…). A possible cause for the differences between JPL-TMF and other stations such as those included in Cooper et al., (2014, 2012) might be related to the different sampling or the differences in the analyzed period. Values in the period 2011-2015, not included in the study by Cooper et al., (2012) seem to strongly contribute to the decreasing trend (see Figure 6). Excluding this years from the analysis and analyzing the same period as in Cooper et al., (2012), we still observe a negative trend at TMF (-0. 07 ppbv.year-1), but it is not statistically significant for this shorter period (p=0.83). These discrepancies between the different studies highlight the strong influence of sampling on the obtained results. Therefore, because of ozone large

variability there is a need for long-term databases which can provide global coverage using homogenous sampling in order to accurately characterized ozone trends in the troposphere as already pointed out in studies such as Lin et al., (2015b).

Comment:
- Sub-section 3.4: This section is the weakest point of the draft paper. My major concern can be summarized as 2 questions: why (only) 8-days backward trajectories ? why (so many) 2-days of residence time over Asia ? These arbitrary choices need further arguments, sensitivity analysis and/or references for similar studies. From my knowledge, Cooper et al, (2010) used 15-days backward trajectories and concluded with a significant influence from Asia to the Western US region, especially in spring. To me, the length of the trajectories used here may be too short and the classification criteria is not adapted, to really assess the different influences authors are looking for. The two plots on Figure 8, bottom row, are too similar to trust in this methodology of classification. The criteria for air masses to be classified as ABL or AFT (at least 2 days over there) is too difficult to meet. What is the reason to impose 2 days over the continent to classify air parcels as "Asian" ? It is way too much. This is probably the reason why the Asian influence does not appear as strong as expected from previous studies. I guess that some (or most of) the air masses classified as Pacific (especially in Spring) would be classified Asian with a different criteria. Results and conclusions may be different with longer trajectories and different criteria for classification. For example, I would suggest to change the order of the sequential attributions: By default, air parcels that are not "stratosphere" would be classified as "Asian" unless the trajectories spend the entire period (8 days or longer) over the Ocean or over Central America. Maybe I'm wrong but I recommend the authors to revise this sub-section to make it convincing. Besides, an interesting information from this analysis of classified air masses would be to check if there is a tendency or anomalous behaviors from one year to another. If I understand well the title and the introduction, this subsection should help further understand the trend analysis. This is not the case so far.

Response:

A sensitivity test was performed to determine the duration of the trajectories and the time residence chosen. Regarding the duration of the trajectories, 8 days was preferred after analyzing trajectories from 5 to 10 days of duration. It was observed that it was time enough to detect the different transport paths we were interested in and 8-day backward trajectories were preferred over longer duration to keep the uncertainty as low as possible, since it increases with the trajectories duration. For the residence time, two days were firstly chosen in order to guarantee that the air masses had enough time to interact with the different ozone sources (e.g. stratosphere, mixing layer above Asia).

However we agree with the reviewer that the chosen parameters were not the most appropriate and the sensitivity test was not exhaustive enough, obtaining misleading results. In this new version of the manuscript, we have performed a more in-depth sensitivity analysis to optimize the residence times over each region and the duration of the trajectories. For this sensitivity test we varied the residence time over each region from 6 to 288 hours (when appropriate) and the duration of the trajectories between 5 and 15 days. Resulting composite ozone profiles, the

number of trajectories and the air masses paths associated to each category were analyzed in detail to optimize the criteria for the classification.

Regarding the duration of the trajectories, this new test reveals that that the composite profiles are not statistically different when using different duration of the trajectories. The main conclusions regarding the ozone mixing ratio values associated to each region are still valid, independently of the trajectories duration (see figure below). However, the number of trajectories associated to each region (included in table 4) do vary significantly, especially for the Asian air masses. For trajectories duration below 10 days, the number of trajectories from Asia is slightly underestimated. A detailed analysis of the trajectories indicates that a value of 12 days for the trajectories significantly improves the results and most of the Asian air masses are correctly identified. Therefore, the trajectories duration has been established at 12 days for the new version of the manuscript. The residence times above each region has been optimized already considering these 12-day backward trajectories.

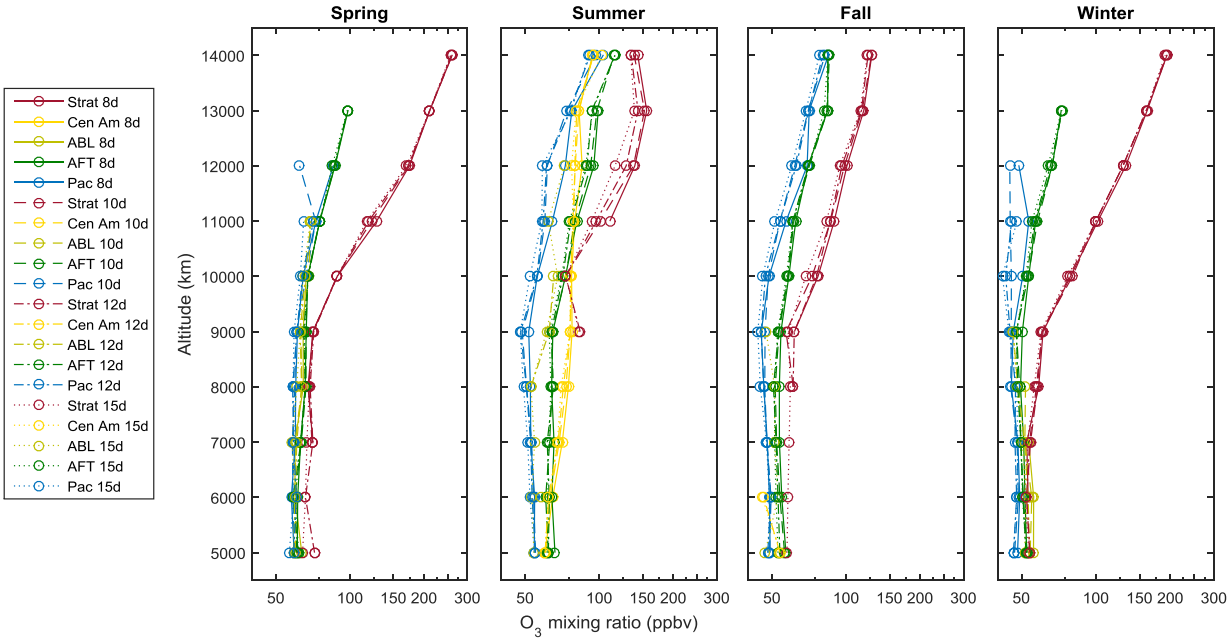

Figure: Composite profiles of the ozone mixing ratio associated with the different categories for each season and for different duration of the trajectories: 8 days (solid line), 10 days (dashed line), 12 days (dot-dash line) and 15 days (dotted line). Results are shown only when the number of samples for a given category was larger than 5% of the total number of samples.

In the case of the stratosphere, a residence time of only six hours already shows the influence of the stratosphere on the profiles, which clearly show increased ozone values. Results are very similar for residence times between 6 and 48 hours. Longer residence time leads to an underestimation of the stratospheric cases, since a large fraction of the trajectories descend to the troposphere after this time. The attached figure shows the average composite profiles obtained varying the residence time for the stratosphere between 6 and 48 hours and the associated standard deviation. As indicated by the low standard deviation, results are not highly dependent on the chosen residence time when selected within this range (6-48 hours). The selection of the

residence time in the stratosphere affects the profiles associated to the other regions, as observed in the figure. The largest standard deviations are associated to the Asian air masses, but variability is still quite low for most of the profiles.

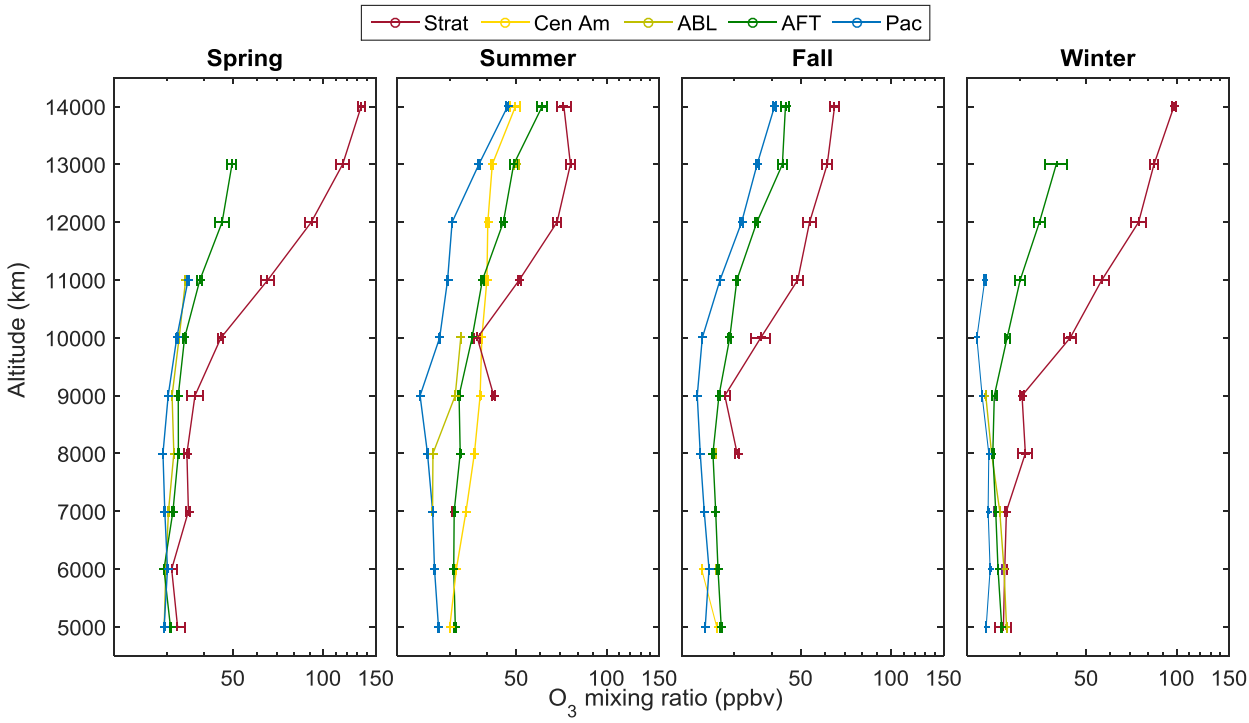

Figure: Mean composite profiles of the ozone mixing ratio associated with the different categories for each season. Error bars are the standard deviation obtained when varying the residence time for the stratosphere between 6 and 48 hours. Residence times for the other categories are fixed (Central America: 96 h, ABL and AFT: 6 h, and Pacific Ocean: 276 h) and the trajectories duration is 12 days. Results are shown only when the number of samples for a given category was larger than 5% of the total number of samples.

In the case of Central America, the residence time has been increased to 96 hours to avoid the influence of additional sources. When lower values were used, air masses coming from Asia were included within the Central America category leading to an overestimation of the number of cases and influencing the ozone values. Larger values of the residence time, on the other hand, lead to an underestimation of the number of cases. Additionally, the Central America region has been slightly extended further north to 40°N. Based on the analysis of the obtained trajectories, this extended region is more adequate to group the trajectories associated to the North American monsoon circulation.

For the Asian air masses, 6 hours residence time is enough to observe the influence of the Asian air masses on the ozone composite profiles. With the new criteria established for the previous regions and duration of the trajectories of 12 days, almost no variation is observed in the ozone values for residence times above Asia between 6 and 48 h hours. However, residence times longer than 6 hours are more restrictive leading to an underestimation of the Asian number of cases. As indicated by the reviewer, residence times of 48 hours for this region with a total

duration of the trajectories of 8 days were too restrictive and the number of Asian cases was strongly underestimated. The manuscript has been modified according to the new results.

The Pacific region includes only those air masses with a residence time larger than 276 hours in the region. That way, influence from additional sources is avoided and this region can be considered as our background region.

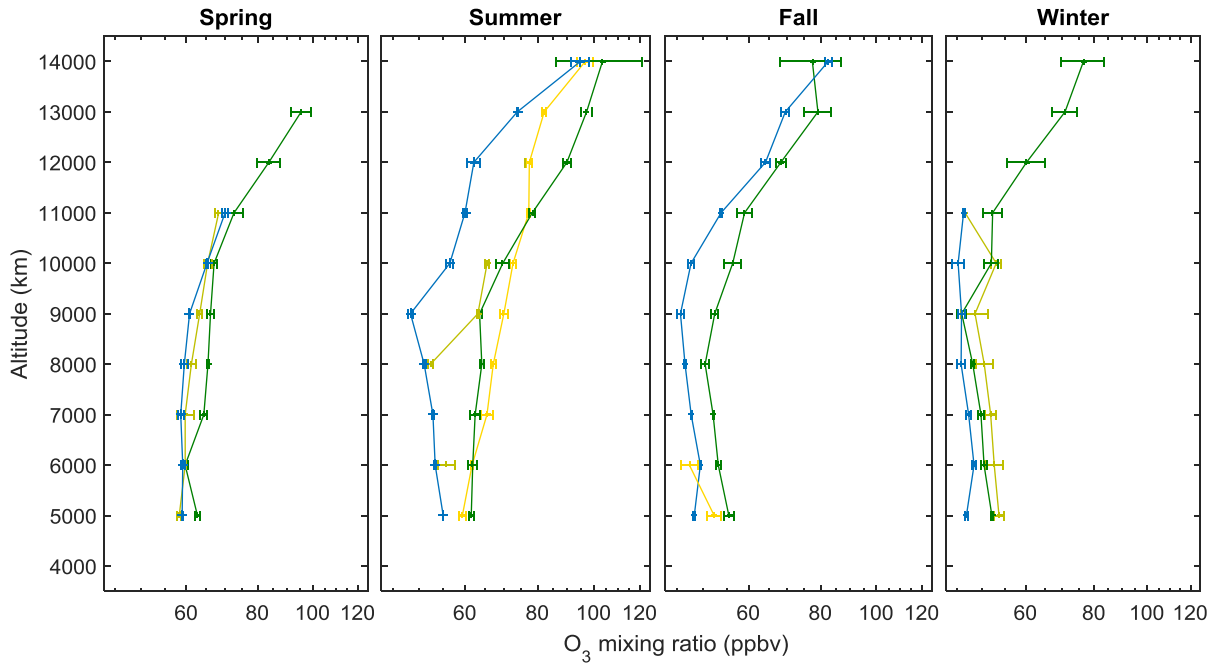

Figure: Mean composite profiles of the ozone mixing ratio associated with the different categories (except for the stratosphere) for each season. Error bars are the standard deviation obtained when varying the residence time for the ABL, AFT, Central America and Pacific regions between 6 and 288 hours. Residence times for the stratosphere are fixed to 12 hours and the trajectories duration is 12 days. Results are shown only when the number of samples for a given category was larger than 5% of the total number of samples.

Trends associated to every region and every season were analyzed, but the number of data is significantly reduced when they are divided in subcategories so no statistically significant results were found, as previously stated. The number of cases associated to each category per year does not show any tendency or anomalous behavior that could explain the interannual variability observed in the profiles (see attached figure). Finally, no significant correlation is found between the number of cases of each category per year and the ozone values either. Even though no significant information on the interannual variability is obtained from the analysis, we think that the information about the different ozone source regions and how they influence the ozone profiles above the site is still quite valuable for the study.

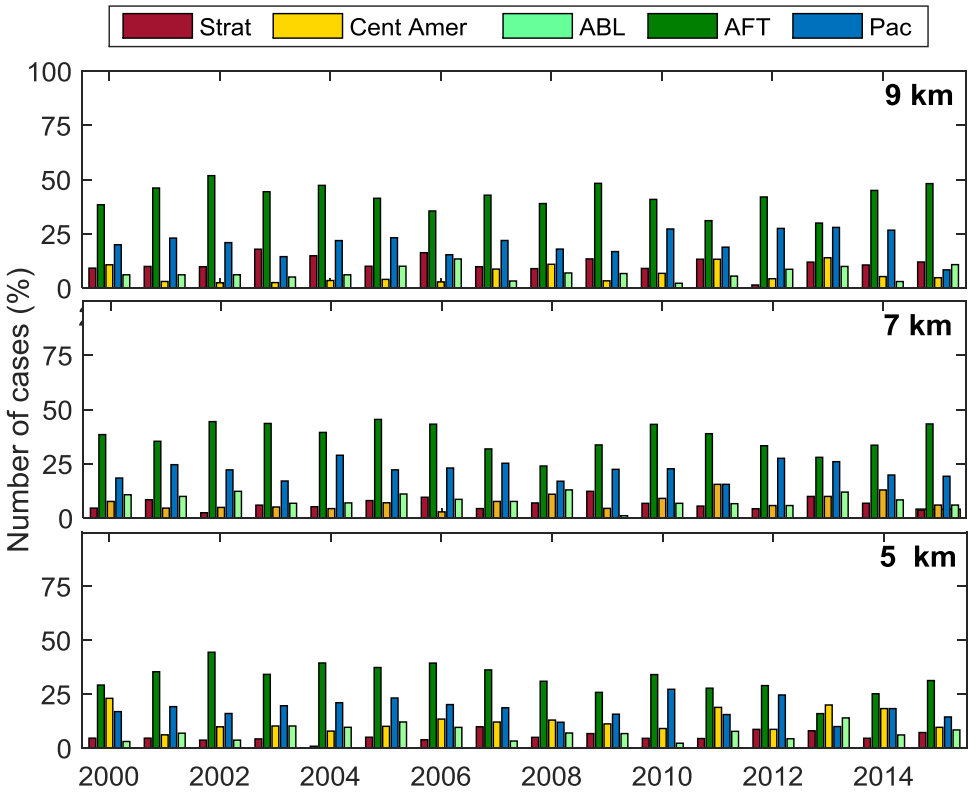

Figure: Number of cases corresponding to every region per year at different altitude levels. The number of cases is normalized to the total number of measurements per year.

Comment:

- Subsection 3.5: A figure showing an individual profiles (not averaged as in Fig.14) with double tropopause would be good to further explain this characteristic to the nonexpert reader. This section should make the distinction clearer between the wording "double tropopause" and "tropopause folds". It is not the same. Sentence line 442-443 and legend of Figure 12 are ambiguous. Indeed, Randel et a., (2007) should be cited as a reference paper for characteristics of double tropopauses.

Response:

An additional figure with an example of tropopause fold has been added to figure 14 and the text has been modified accordingly.

Text has also been modified to make a clearer distinction between "double tropopause" and "tropopause fold". The following text has been added to the manuscript:

Lines 513-516: *"Double tropopauses are usually expected to result from tropopause folds in the layer between the two identified tropopauses. Therefore, a common method used in the literature*

to identify tropopause folds is to detect the presence of double tropopauses based on temperature profiles (e.g. Chen et al., 2011).”

The reference Randel et al., (2007) has been included where appropriate.

Comment:

- Section 4: This section is a bit too long. It starts like a summary but then includes analysis and explanations that would be better placed before in the associated subsections. More importantly, some highlighted discussions are mentioned as in contradiction with other studies without any further discussions. This needs to be further argued. For example : - Line 477-484: Either the comparison with recent findings by Lin et al., (2015) and Neu et al., (2014) makes senses and the inconsistency raises important questions (i.e., what makes JPL-TMF station different and not representative of the general behavior ?), or the comparison is not possible (need to explain why ?) and such paragraph is simply to be removed.

Response:

Section 4 has been removed and discussion is now included under the corresponding results in section 3.

The comparison with Lin et al., (2015) and Neu et al., (2014) has been removed since a simple interpretation is not possible due to the different characteristics of the datasets. Their results refer to a wider region and column-integrated data, whereas we have a single site with different temporal and vertical sampling. Therefore, a straightforward comparison is not likely and this sentence can lead to uncertain interpretations.

- Lines 498-503: This negative trend in winter observed at JPL-TMF is surprising, in contradiction with most of the studies I’m aware of, and therefore deserves further investigations. According to Cooper et al., (2012) only one site in the Western US shows negative trend in winter, and only for the 95% percentile. This is different from what is presented in Table 2 in this study. “Decrease in background ozone during these months : : : ” is definitely an opposite conclusion to that of Cooper et al., (2012) and of similar recent studies. As for previous comment, I recommend the authors to answer the question “why do JPL-TMF measurements highlight different behaviors ?”

Response:
The sentence “Decrease in background ozone during these months…” has been removed.
As previously explained, differences between our results and previous studies might be due to differences in sampling and the different analyzed period compared to Cooper et al., (2012). Possible causes for the decreasing trend in winter have been investigated, but no significant results that can satisfactorily explain this trend were obtained. According to sections 3.4 and 3.5, an important source of ozone during winter would be the stratosphere, but no significant trends

for the ozone values associated to the stratospheric air masses were found in winter. No anomalous behavior or significant decrease in the number of stratospheric cases was observed during the analyzed period. The same results were obtained for the Asian air masses and the tropopause folds data during winter. It is worthy to note that the number of data is significantly reduced when they are subdivided in seasons and in the different categories associated to the five regions considered in the trajectories analysis, affecting the significance of the results. A combination of the lidar database with additional data (e.g. model, satellite, additional stations…) would be necessary to reach significant conclusions in this respect.

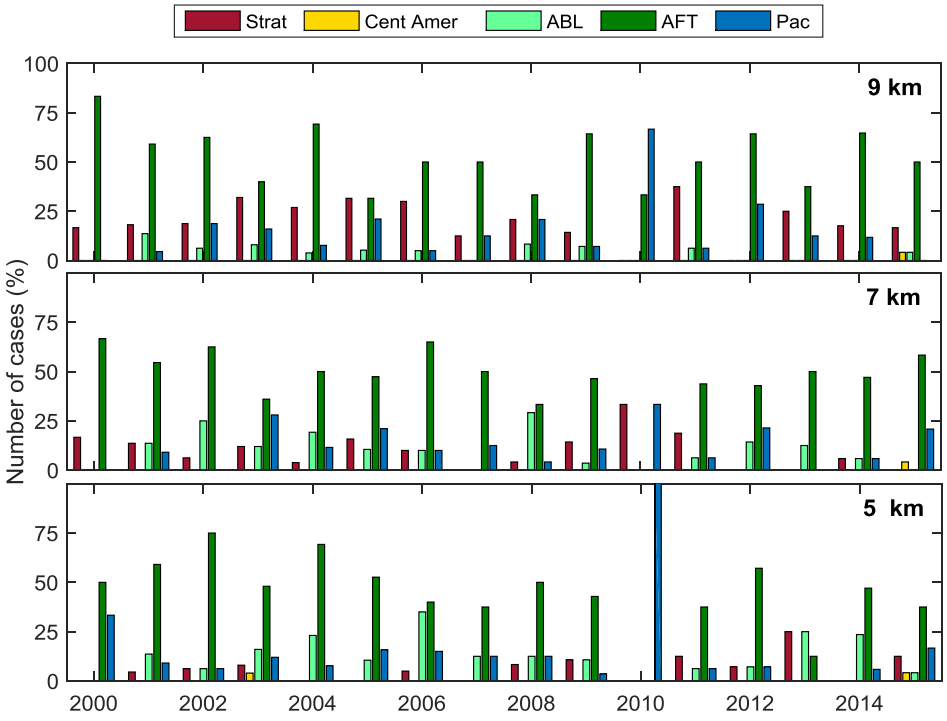

Figure: Number of cases corresponding to every region per year at different altitude levels in winter. The number of cases is normalized to the total number of measurements per year in winter.

Comment:
- Line 513-517: Wouldn't it be good to have results from this extended analysis ?

Response:
This study is undergoing and robust and reliable results are not yet available to be published. The sentence has been removed.

Minor comments :
- Line 61 : "directly emitted" seems to me too ambiguous and may let the reader think that ozone is a primary pollutant. I suggest to replace by "transported down from the stratosphere".

This part has been modified according to both reviewers' suggestions.

Lines 64-65: *"Tropospheric ozone is primarily formed as a secondary pollutant in chemicals reactions involving ozone precursors such as methane, CO, NOx, VOCs or PANs."*

- Line 88-89 : I suggest to remove the end of the sentence starting at "which has not yet been : : :" because this not true, as written indeed in the following paragraph.

The sentence has been rewritten:

Lines 96-99: *"In the last decades, efforts have been made in this respect and the number of tropospheric ozone measurements has considerably increased throughout the globe. However, it is still necessary to increase the current observation capabilities to characterize tropospheric ozone variability more accurately."*

- Line 285-286: Do R=0.34 or 0.44 really show correlation?

This paragraph has been removed considering both reviewers' comments.

- Line 287-290: This is more interesting than the lines before and deserves a brief explanation. Why outliers have to be removed to confirm the correlation. Does this tell us something on specific process at the surface or at 4-6 km altitude? Is there different disconnected influences ? For a specific season?

A first quick analysis reveals that outliers are mostly related to different ozone sources affecting the surface and the layer at 4-6 km. For example, stratospheric air going down to 4-6 km and not reaching the surface or local ozone production related to anthropogenic emissions near JPL-TMF site for those cases when the boundary layer reaches the station. However, the database available is not large enough to obtain significant and robust conclusions since surface data are available only since 2013. Especially, the number of cases is very low to try to identify any seasonal variation. According to both reviewers' comments on this section it has been removed from the manuscript.

- Figure 5: I am wondering if the choice of the color sale is the most appropriate to highlight (real and significantly positive or negative) anomalies. What about choosing a color scale centered on 0 (same color for -10 to +10) ? It is difficult to check consistency with Figure 6. Is there any explanation for long-lasting anomalies in 2003-2007 ?

Comparison between figure 6 and 7 is not straightforward since the first one shows monthly deviations from the climatological values in percentage and figure 6 is based on yearly median values expressed in ppbv for certain layers. We think that the use of the same color for positive and negative values suggested by the reviewer would mean a loss of information regarding the positive and negative anomalies.
Regarding the long-lasting positive anomalies in 2003-2007, we analyzed correlation with global circulation patterns such as ENSO or the QBO to identify the causes of the anomalies in 2003-2007, but no significant influence was observed. Additionally, a significant higher influence of any of the air masses from the five considered categories in Section 3.4 (Stratosphere, Central

America, ABL, AFT and Pacific) or the tropopause folds in Section 3.5 was not detected during this period.

- Line 341: This reference is missing in the list.

We apologize for the mistake. Reference has been added to the list.
Engström, A. and Magnusson, L.: Estimating trajectory uncertainties due to flow dependent errors in the atmospheric analysis, Atmos. Chem. Phys., 9, 8857–8867, doi:10.5194/acp-9-8857-2009,2009.

- Line 412-414: This sentence needs to be accompanied by a reference to give argument that an excess of 15 ppbv is what is expected as lightning-induced enhancement of ozone. Is Cooper et al. (2009) as mentioned in section 4 (line 537) relevant for this ?

The different between the ozone associated to the air masses classified as Central America and the Pacific Ocean is now 20 ppbv based on the new analysis in Section 3.4. We do not mean to attribute this ozone excess for the Central America air masses exclusively to lightning-induced enhancement of ozone. The sentence is meant to highlight that we have higher ozone mixing ratio values when air masses are coming from Central America. Cooper et al., (2009) shows an increased value of NOx based on models above JPL-TMF associated to lightning during the North American Monsoon but does not provide a corresponding ozone value. Lightning-induced NOx is an ozone precursor and the larger ozone values associated to Central American masses observed in our study seem to be the result of local ozone production associated to this enhanced NOx production. However, with the methodology used in this study an accurate quantification of the ozone associated to lightning is not possible. The use of chemical transport models would be required for that quantification. The possibility of a fraction of this ozone associated to different sources such as transport from Central America or even mixing with different sources such as the stratosphere cannot be ignored. Text has been modified to avoid confusion.

- Line 429: MERRA acronym needs to be explained. Reference would be nice.

Lines 516-518: *"The MERRA (Modern-Era Retrospective analysis for Research and Applications, Rienecker et al., 2011) reanalysis data (1-km vertical resolution, 1 x 1.25 degrees horizontal resolution) were used in this study to identify the presence of double tropopauses above the station."*

- Reference list:

The following references are incomplete :

Ambrose et al., 2011; Cooper and Stohl, 2005; Lee and Akimoto, 1998; Monks, 2005; Petetin et al., 2015 (should check if ACP reference is available).

References :
Cooper, O. R., Stohl, A., Eckhardt, S., Parrish, D. D., Oltmans, S. J., Johnson, B. J., Nédélec P., Schmidlin, F. J., Newchurch, M. J., Kondo, Y., and Kita, K.: A springtime

comparison of tropospheric ozone and transport pathways on the east and west coasts of the United States, J. Geophys. Res., 110, D05S90, doi: 10.1029/2004JD005183, 2005.
Jaffe, D., Price, H., Parrish, D., Goldstein, A., and Harris, J.: Increasing background ozone during spring on the west coast of North America, Geophys. Res. Lett., 30, 1613, doi:10.1029/2003GL017024, 2003.

Logan J.A., J. Staehelin, I. A. Megretskaia, J.-P. Cammas, V. Thouret, H. Claude, H. De Backer, M. Steinbacher, H. E. Scheel, R. Stübi, M. Fröhlich, and R. Derwent, Changes in ozone over Europe since 1990: analysis of ozone measurements from sondes, regular aircraft (MOZAIC) and alpine surface sites. J. Geophys. Res., D09301, doi:10.1029/2011JD016952, 2012.

Neuman, J. A., Trainer, M., Aikin, K. C., Angevine, W. M., Brioude, J., Brown, S. S., de Gouw, J. A., Dube, W. P., Flynn, J. H., Graus, M., Holloway, J. S., Lefer, B. L., Nedelec, P., Nowak, J. B., Parrish, D. D., Pollack, I. B., Roberts, J. M., Ryerson, T. B., Smit, H., Thouret, V., and Wagner, N. L.: Observations of ozone transport from the free troposphere to the Los Angeles basin, J. Geophys. Res., 117, D00V09, doi: 10.1029/2011JD016919, 2012.

Parrish, D., Dunlea, E. J., Atlas, E. L., Schauffler, S., Donnelly, S., Stroud, V., Goldstein, A. H., Millet, D. B., McKay, M., Jaffe, D. A., Price, H. U., Hess, P. G., Flocke, F., and Roberts, J. M.: Changes in the photochemical environment of the temperate North Pacific troposphere in response to increased Asian emissions, J. Geophys. Res., 109, D23S18, doi: 10.1029/2004JD004978, 2004.

Randel, W. J., D. J. Seidel, and L. L. Pan, Observational characteristics of double tropopauses, J. Geophys. Res., 112, D07309, doi:10.1029/2006JD007904, 2007.

Zbinden R.M., V. Thouret, P. Ricaud, F. Carminati, J.-P. Cammas, and P. Nédélec, Climatology of pure tropospheric profiles and column contents of ozone and carbon monoxide using MOZAIC in the mid-northern latitudes (24_ N to 50_ N) from 1994 to 2009„ Atmos. Chem. Phys., 13, 12363-12388, doi:10.5194/acp-13-12363-2013, 2013.

References has been modified.

 # Response to Mike Newchurch

Interactive comment on "Tropospheric Ozone Seasonal and Long-term Variability as seen by lidar and surface measurements at the JPL-Table Mountain Facility, California" by M. J. Granados-Muñoz and T. Leblanc

M. J. Newchurch (Referee)
mike@nsstc.uah.edu
Received and published: 2 May 2016

General Comments:
This paper is a very useful contribution to the rather limited literature of the vertical distribution of ozone over the USA west coast. The analytical techniques employing trajectory analysis, stratospheric-tropospheric folding dynamical structures, time series and variability analysis, and attribution analysis all contribute to the value of this work. The major shortcomings concern the choices for trajectory/attribution parameters (primarily time scales) and the absence of a concise conclusion section. Minor shortcomings concern the details of the trend analysis and some inconsistencies in the attribution. This paper should be accepted after these issues are successfully addressed.

Response:

First of all, we would like to thank the reviewer for the comments and suggestions which have helped to improve the quality of the manuscript. Especially, section 3.4 is now much improved and more significant results were found. Comments and suggestions have been really helpful to improve the section and the quality of the manuscript.

The trajectories attribution section has been modified considering the suggestions and comments from both reviewers. An in-depth sensitivity analysis to optimize the residence times over each region and the duration of the trajectories has been performed and new criteria have been established. Additional details on the selection of the parameters and the duration of the trajectories are now included in the manuscript. More information is provided next.

For the sensitivity test we varied the residence time over each region from 6 to 288 hours (when appropriate) and the duration of the trajectories between 5 and 15 days. Resulting composite ozone profiles, the number of trajectories and the air masses paths associated to each category were analyzed in detail to optimize the criteria for the classification.

Regarding the duration of the trajectories, the sensitivity test reveals that that the composite profiles are not statistically different when using different duration of the trajectories. The main conclusions regarding the ozone mixing ratio values associated to each region are still valid, independently of the trajectories duration (see figure below). However, the number of trajectories associated to each region (included in table 4 in the manuscript) do vary significantly, especially for the Asian and Pacific air masses. For trajectories duration below 10 days, the number of trajectories from Asia is slightly underestimated. A detailed analysis of the trajectories indicates that a value of 12 days for the trajectories significantly improves the results and most of the

Asian air masses are correctly identified. Therefore, the trajectories duration has been established at 12 days for the new version of the manuscript. The residence times above each region has been optimized already considering these 12-day backward trajectories.

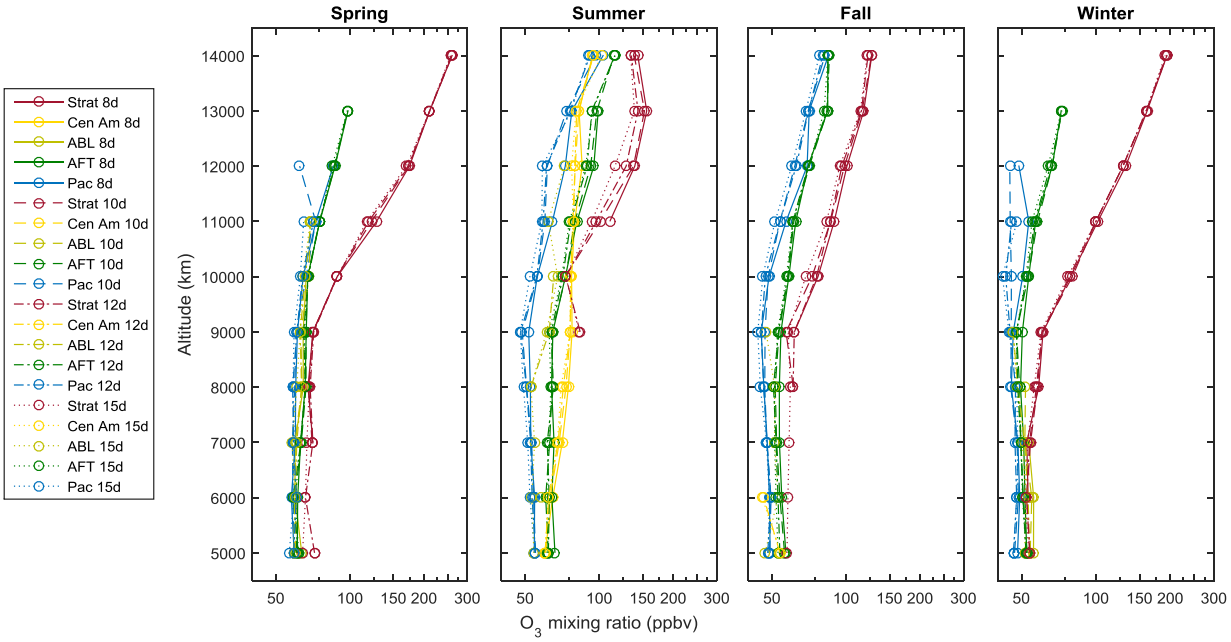

Figure: Composite profiles of the ozone mixing ratio associated with the different categories for each season and for different duration of the trajectories: 8 days (solid line), 10 days (dashed line), 12 days (dot-dash line) and 15 days (dotted line). Results are shown only when the number of samples for a given category was larger than 5% of the total number of samples.

In the case of the stratosphere, a residence time of only six hours already shows the influence of the stratosphere on the profiles, which clearly show increased ozone values. Results are very similar for residence times between 6 and 48 hours. Longer residence time leads to an underestimation of the stratospheric cases, since a large fraction of the trajectories descend to the troposphere after this time. The attached figure shows the average composite profiles obtained varying the residence time for the stratosphere between 6 and 48 hours and the associated standard deviation. As indicated by the low standard deviation, results are not highly dependent on the chosen residence time when selected within this range (6-48 hours). The selection of the residence time in the stratosphere affects the profiles associated to the other regions, as observed in the figure. The largest standard deviations are associated to the Asian air masses, but variability is still quite low for most of the profiles.

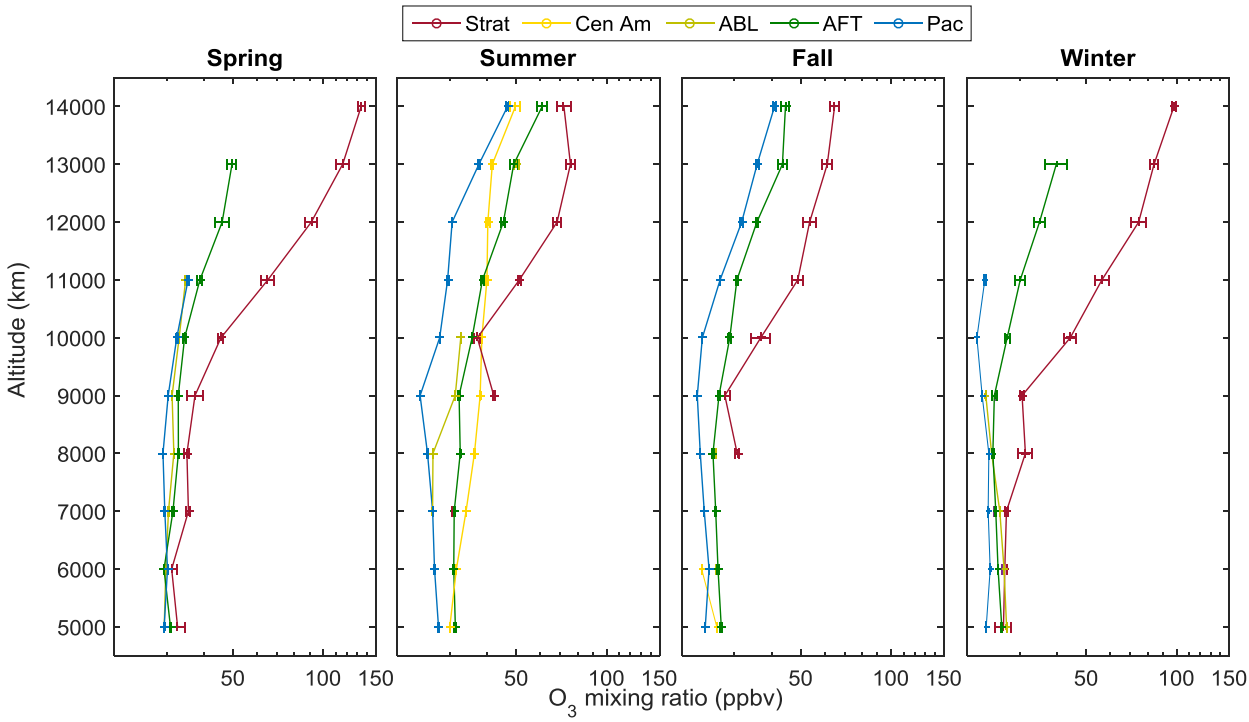

Figure: Mean composite profiles of the ozone mixing ratio associated with the different categories for each season. Error bars are the standard deviation obtained when varying the residence time for the stratosphere between 6 and 48 hours. Residence times for the other categories are fixed (Central America: 96 h, ABL and AFT: 6 h, and Pacific Ocean: 276 h) and the trajectories duration is 12 days. Results are shown only when the number of samples for a given category was larger than 5% of the total number of samples.

In the case of Central America, the residence time has been increased to 96 hours to avoid the influence of additional sources. When lower values were used, air masses coming from Asia were included within the Central America category leading to an overestimation of the number of cases and influencing the ozone values. Larger values of the residence time, on the other hand, lead to an underestimation of the number of cases. Additionally, the Central America region has been slightly extended further north to 40°N. Based on the analysis of the obtained trajectories, this extended region is more adequate to group the trajectories associated to the North American monsoon circulation.

For the Asian air masses, 6 hours residence time is enough to observe the influence of the Asian air masses on the ozone composite profiles. With the new criteria established for the previous regions and duration of the trajectories of 12 days, almost no variation is observed in the ozone values for residence times above Asia between 6 and 48 h hours. However, residence times longer than 6 hours are more restrictive leading to an underestimation of the Asian number of cases. Residence times of 48 hours for this region with a total duration of the trajectories of 8 days were too restrictive and the number of Asian cases was strongly underestimated. The manuscript has been modified according to the new results.

The Pacific region includes only those air masses with a residence time larger than 276 hours in the region. That way, influence from additional sources is avoided and this region can be considered as our background region.

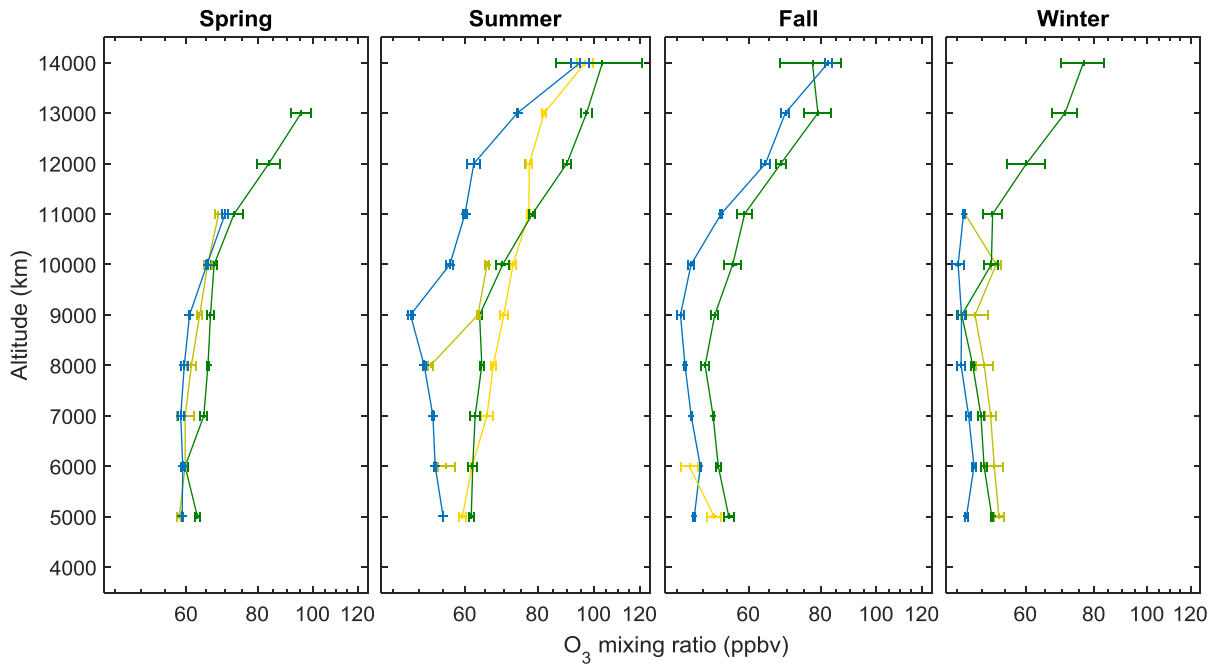

Figure: Mean composite profiles of the ozone mixing ratio associated with the different categories (except for the stratosphere) for each season. Error bars are the standard deviation obtained when varying the residence time for the ABL, AFT, Central America and Pacific regions between 6 and 288 hours. Residence times for the stratosphere are fixed to 12 hours and the trajectories duration is 12 days. Results are shown only when the number of samples for a given category was larger than 5% of the total number of samples.

A conclusion sections was already added to the manuscript published in ACPD. Please note that the version published and the version attached by the reviewer as a supplement are different. The conclusions section has now been modified in the new version of the manuscript according to the new results obtained in Section 3.4.

Specific Comments: L36: 'No outstanding influence from Asia was identified'. This absence of Asian influence is strongly dependent on the somewhat arbitrary selection of trajectory time-scale parameters. This conclusion is also somewhat inconsistent with the early spring maximum in figure 4. Consider additional analyses to resolve this discrepancy by providing compelling evidence to support your finding.

Response:

We agree with the reviewers that the chosen parameters in Section 3.4 were not the most appropriate and the sensitivity test performed was not exhaustive enough, obtaining misleading results. As previously explained, a new analysis has been performed based on a more exhaustive sensitivity analysis to optimize the residence times over each region and the duration of the trajectories. The new criteria used in the back-trajectories analysis section reveal now the influence of air masses coming from Asia on the ozone profiles measured at JPL-TMF and results are in agreement with previous studies. The manuscript has been modified accordingly.

L44: 'Tropospheric ozone can be directly emitted to the troposphere, ': Direct emissions (separate from STE injections) are a very small fraction of tropospheric ozone sources. Suggest you omit this sentence.

Response:
Sentence has been removed.

L273: Removing data +/- 1 sd for a correlation calculation is not a legitimate approach. That process will remove approximately 1/3 of the data and will certainly enhance the correlation between the remaining data, but one cannot justify removing that many data and one would certainly not call all those data 'outliers'.

Response:
This paragraph has been omitted from the manuscript considering both reviewers' concerns.

L296: Suggest you use p-values of 0.05 to be consistent with the 95% statistics used elsewhere.

Response:
A discussion using p-Values of 0.05 is also included to be consistent and ease comparison with previous studies. Nonetheless, the criterion of p-Values lower than 0.1 is also used in atmospheric sciences (e. g. Xia et al., 2008; Wilson et al., 2012) and we consider it is worthy to maintain it in the study. A confidence level larger than 90% is still quite significant and these trends should not be neglected. Tables and text has been modified accordingly.

Xia, X., T. F. Eck, B. N. Holben, G. Phillippe, and H. Chen (2008), Analysis of the weekly cycle of aerosol optical depth using AERONET and MODIS data, J. Geophys. Res., 113, D14217, doi:10.1029/2007JD009604.

Wilson, R. C., Fleming, Z. L., Monks, P. S., Clain, G., Henne, S., Konovalov, I. B., Szopa, S., and Menut, L.: Have primary emission reduction measures reduced ozone across Europe? An analysis of European rural background ozone trends 1996–2005, Atmos. Chem. Phys., 12, 437-454, doi:10.5194/acp-12-437-2012, 2012.

Section 4: The summary should be expressed in the Abstract. No need for another summary here. The more discussions should be moved to the section under discussion or a new section heading inserted. The paper needs a short 'Conclusions' section (not summary or discussion). The conclusions should be succinct and describe the main take-home points derived from the paper.

Response:
The discussions have been inserted in Section 3 with the corresponding results as suggested by Reviewer 1. Therefore the discussion section is no longer included in the manuscript.

Technical corrections: See attached .docx for suggested tracked changes.
Please also note the supplement to this comment:

http://www.atmos-chem-phys-discuss.net/acp-2016-70/acp-2016-70-RC2-supplement.pdf

Response:
Technical corrections suggested by the reviewer have been addressed in the new version of the manuscript.
Regarding the comment on Line 500 (The wintertime negative results require an explanation), additional details has been added to explain the discrepancies with previous studies. A possible cause for the differences between JPL-TMF and other stations such as those included in Cooper et al., (2014, 2012) might be related to the different sampling or the differences in the analyzed period. Values in the period 2011-2015, not included in the study by Cooper et al., (2012) seem to strongly contribute to the decreasing trend (see Figure 6). Excluding this years from the analysis and analyzing the same period as in Cooper et al., (2012), we still observe a negative trend at TMF (-0. 07 ppbv.year^{-1}), but it is not statistically significant for this shorter period (p=0.83). These discrepancies between the different studies highlight the strong influence of sampling on the obtained results, as already suggested in Lin et al., (2015b). Possible causes for the decreasing trend in winter have been investigated, but no significant results that can satisfactorily explain this trend were obtained. According to sections 3.4 and 3.5, an important source of ozone during winter would be the stratosphere, but no significant trends for the ozone values associated to the stratospheric air masses were found in winter. No anomalous behavior or significant decrease in the number of stratospheric cases was observed either during the analyzed period. The same results were obtained for the Asian air masses and the tropopause folds data during winter. It is worthy to note that the number of data is significantly reduced when they are subdivided in seasons and in the different categories associated to the five regions considered in the trajectories analysis, affecting the significance of the results. A combination of the lidar database with additional data (e.g. model, satellite, additional stations…) would be necessary to reach significant conclusions in this respect.

Manuscript with tracked changes:

Tropospheric Ozone Seasonal and Long-term Variability as seen by lidar and surface measurements at the JPL-Table Mountain Facility, California

Maria Jose Granados-Muñoz[1] and Thierry Leblanc[1]

1 Jet Propulsion Laboratory, California Institute of Technology, Wrightwood, CA, USA

Corresponding author: mamunoz@jpl.nasa.gov

Keywords: NDACC, lidar, ozone, troposphere, surface ozone, TOLNet, long-term, tropopause folds, UTLS

Abstract

A combined surface and tropospheric ozone climatology and interannual variability study was performed for the first time using co-located ozone photometer measurements (2013-2015) and tropospheric ozone differential absorption lidar measurements (2000-2015) at the Jet Propulsion Laboratory Table Mountain Facility (TMF, elev. 2285 m), in California.

The surface time-series were investigated both in terms of seasonal and diurnal variability. The observed surface ozone is typical of high-elevation remote-sites, with small amplitude of the seasonal and diurnal cycles, and high ozone values, compared to neighboring lower altitude stations representative of urban boundary layer conditions. The ozone mixing ratio ranges from 45 ppbv in the winter morning hours to 65 ppbv in the spring and summer afternoon hours. At the time of the lidar measurements (early night), the seasonal cycle observed at the surface is similar to that observed by lidar between 3.5 km and 9 km.

Above 9 km, the local tropopause height variation with time and season impacts significantly the ozone lidar observations. The frequent tropopause folds found in the vicinity of TMF (27% of the time, mostly in winter and spring) produce a dual-peak vertical structure in ozone within the fold layer, characterized by higher-than-average values in the bottom half of the fold (12-14 km), and lower-than-averaged values in the top half of the fold (14-18 km). This structure is consistent with the expected origin of the air parcels within the fold, i.e., mid-latitude stratospheric air folding down below the upper tropospheric sub-tropical air. The influence of the tropopause folds extends down to 5 km, increasing the ozone content in the troposphere.

No significant signature of interannual variability could be observed on the 2000-2015 deseasonalized lidar time-series, with only a statistically non-significant positive anomaly during the years 2003-2007. Our trend analysis reveals however an overall statistically significant positive trend of 0.3 ppbv.year^{-1} (0.6%) in the free troposphere (7-10km) for the period 2000-2015.

A classification of the air parcels sampled by lidar was made at 1-km intervals between 5 km and 14 km altitude, using 12-day backward trajectories (HYSPLIT). Our classification revealed the influence of the Pacific Ocean, with air parcels of low ozone content (43-60 ppbv below 9 km), and significant influence of the stratosphere leading to ozone values of 57-83 ppbv down to 8-9 km. In summer, enhanced ozone values (76 ppbv at 9 km) were found in air parcels originating from Central America, probably due to the enhanced thunderstorm activity during the North American Monsoon. ~~No outstanding influence from Asia was identified.~~ Influence from Asia was observed throughout the year, with more frequent episodes during spring, associated to ozone values from 53 to 63 ppbv at 9 km.

1. Introduction

Ozone is an important constituent in the troposphere, impacting climate, chemistry, and air quality (The Royal Society, 2008). As a greenhouse gas (Forster et al., 2007), it contributes to the Earth's global warming with an estimate radiative forcing of 0.40 ± 0.20 W·m^{-2} (IPCC 2013). It is one of the main oxidants in the troposphere (Monks, 2005), and, in high concentrations, it can cause problems in human health and vegetation (World Health Organization, 2003). Tropospheric ozone ~~can be directly emitted to the troposphere, but it~~ is primarily formed as a secondary pollutant in chemicals reactions involving ozone precursors such as methane, CO, NOx, VOCs or PANs. An additional source of ozone in the troposphere is the downward transport from the stratosphere, where ozone is much more abundant (Levy et al., 1985). At high elevation sites such as the Jet Propulsion Laboratory Table Mountain Facility in Southern California (TMF hereafter), the effect of the boundary layer is very small, and ozone variability is expected to be driven by transport processes from the stratosphere or horizontal transport within the troposphere (Cui et al., 2009; Naja et al., 2003; Trickl et al., 2010).

Several studies show that background ozone levels have increased significantly since preindustrial times (Mickley et al., 2001; Parrish et al., 2012; Staehelin et al., 1994; Volz and Kley, 1988) and these levels continued rising in the last decades in both Hemispheres (Derwent et al., 2007; Jaffe et al., 2004; Lee and Akimoto, 1998; Naja and Akimoto, 2004; Oltmans et al., 2006; Parrish et al., 2012; Simmonds et al., 2004; Tanimoto et al., 2009; Zbinden et al., 2006; Lelieveld et al., 2004). Nevertheless, after air quality regulations were implemented in the 1970s, the increasing trend has slowed down or is even reversed in regions such as the Eastern U.S. and Europe (Cooper et al., 2012, 2014; Granier et al., 2011). The situation is not the same for emerging economies such as Asia, where emissions are increasing with a corresponding increase in ozone levels (Dufour et al., 2010; Gao et al., 2005; Strode et al., 2015; Tie et al., 2009; Wang et al., 2006).

In most cases, variability and trend studies have revealed very large ozone variability with time, location and altitude (Cooper et al., 2014). This variability is mostly due to the large heterogeneity and variability of the ozone sources themselves, the different chemical processes affecting the formation and depletion of tropospheric ozone and its variable lifetime in the troposphere. Ozone atmospheric lifetime goes from a few hours in polluted boundary layer to

several weeks in the free troposphere, allowing it to travel over distances of intercontinental scale (Stevenson et al., 2006; Young et al., 2013). Additional factors that have been observed to influence tropospheric ozone variability are climate variability and related global circulation patterns such as ENSO or PDO (e.g. Lin et al., 2014; 2015a; Neu et al., 2014). Tropopause folds also play a key role on tropospheric ozone interannual variability, as they influence the ozone budget in the troposphere and can even affect air quality near the surface (e.g. Lin et al., 2015a Brown-Steiner and Hess, 2011; Langford et al., 2012). In order to obtain statistically significant results and be able to assess tropospheric ozone interannual variability and trends, a large long-term monitoring dataset with global coverage is required. In the last decades, efforts have been made in this respect and the number of tropospheric ozone measurements has considerably increased throughout the globe. However, it is still necessary to increase the current observation capabilities to characterize tropospheric ozone variability more accurately ~~which has not yet been achieved considering the current observation capabilities.~~

Long-term records of tropospheric ozone are available since the 1950s (Feister and Warmbt, 1987; Parrish et al., 2012), but it is not until the 1970s that the number of ozone monitoring stations became significant (Cooper et al., 2014 and references therein). Currently, a considerable number of ozone monitoring sites are operating as part of regional networks or international programs (e.g. World Meteorological Observation Global Atmosphere Watch WMO/GAW, Acid Deposition Monitoring Network in East Asia EANET, Clean Air Status and Trends Network CASTNET, etc.). In addition to these ground-based networks, tropospheric ozone measurements from satellite (TOMS, TES, OMI, etc.) or aircraft (MOZAIC/IAGOS) platforms have been successfully implemented. Nevertheless, a large fraction of the tropospheric ozone measurements are still only surface or column-integrated measurements whilst the number of them with information on the vertical coordinate is very small. Until recently, mainly ozonesonde profiles have been used to provide altitude-resolved ozone variability information in the troposphere (Logan, 1994; Logan et al., 1999; Naja and Akimoto, 2004; Oltmans et al., 1998, 2006, 2013; Newchurch et al., 2003), but the ~~somewhat elevated~~ cost of an ozonesonde launch has kept the sampling interval to one profile per week (or less) for a given location. Ozone vertical profiles have also been obtained from aircraft platforms through programs such as MOZAIC and IAGOS, available since 1995 (e.g. Zbinden et al., 2013, Logan et al., 2012). However, aircraft data are limited to air traffic routes and the temporal resolution depends on the

frequency of the commercial flights. Differential Absorption Lidar (DIAL) systems, which started to be used to measure tropospheric ozone in the late 1970s (Bufton et al., 1979; Proffit and Langford, 1997), complement the ozonesonde and aircraft records, providing higher temporal resolution thanks to their inherent operational configuration (from minutes to days of continuous measurements). Currently, tropospheric ozone lidars are still very scarce, but the implementation of observation networks such as the international Network for the Detection of Atmospheric Composition Change (NDACC, http://www.ndsc.ncep.noaa.gov), and more recently the North American-based Tropospheric Ozone Lidar Network (TOLNet, http://www-air.larc.nasa.gov/missions/TOLNet) allows for new capabilities that can contribute to the understanding of processes affecting tropospheric ozone variability, and to satellite and model validation and improvement.

As part of NDACC and TOLNet, a tropospheric ozone DIAL system located at TMF has been operating since 1999. In this study, an analysis of 16 years of lidar profiles measured at the station is presented together with the analysis of the surface ozone measurements available at the site since 2013. The objective is to provide the first-ever published study of tropospheric ozone variability above TMF using both the surface and lidar datasets. The work presented here is particularly valuable due to the rising interest in the detection of long-term trends in the Western United States (U.S.) and the scarcity of long-term measurements of ozone vertical profiles in this region. The high-terrain elevation and the deep planetary boundary layer of the intermountain Western U.S. region facilitate inflow of polluted air masses originating in the Asian boundary layer and ozone-rich stratospheric air down to the surface, thus highly influencing air quality in the region (Brown-Steiner and Hess, 2011; Cooper et al., 2004; Langford et al., 2012; Liang et al., 2004; Lin et al., 2012a, 2012b; Stohl, 2002). After a brief description of the instrumentation and datasets (Section 2), an analysis of the seasonal and interannual variability of tropospheric ozone above TMF for the period 2000-2015 will be presented in section 3. The study includes a characterization of the air parcels sampled by lidar by identification of the source regions based on backward trajectories analysis. Concluding remarks are provided in Section 4.

2. Instrumentation

2.1 Tropospheric ozone lidar

TMF is located in the San Gabriel Mountains, in Southern California (34.4◦ N, 117.7◦ W), at an elevation of 2285 m above sea level. Two differential absorption lidars (DIAL) and one Raman lidar have been operating at the facility during nighttime typically four times per week, two hours per night, contributing stratospheric ozone, temperature, tropospheric ozone, and water vapor measurements to NDACC for several decades now. The original design in the mid-1990s of the tropospheric ozone DIAL was optimized for tropospheric ozone and aerosol measurements (McDermid, 1991). The system was later re-designed to provide exclusively tropospheric ozone profiles (McDermid et al., 2002). The emitter uses a quadrupled Nd:YAG laser emitting two beams at 266 nm. One beam passes through a Raman cell filled with Deuterium to shift the wavelength to 289 nm, the other beam passes through another cell filled with Hydrogen to shift the wavelength to 299 nm. The two beams are then expanded five times and transmitted into the atmosphere. The light elastically backscattered in the troposphere (3-20 km) is collected by three (later five) telescopes comprising mirrors of diameters varying from 91 cm diameter to 5 cm diameter, thus accommodating for the large signal dynamic range occurring when collecting light from this close range. A total of three pairs of 289/299 nm channels is thus used to retrieve ozone using the DIAL technique, each pair corresponding to a different intensity range and the retrieved ozone profiles from all pairs combined ~~together~~ ultimately covers the entire troposphere (3-18 km). As part of the retrieval process, the upper range of the ozone profile is further extended to about 25 km by applying the DIAL technique on the 299 nm high intensity channel of the tropospheric ozone lidar and the 355 nm low-intensity channel of the co-located water vapor Raman lidar (Leblanc et al., 2012).

The instrument temporal sampling can be set to any value from a few seconds to several hours and the vertical sampling can be set to any multiple of 7.5 m, depending on the science or validation need. ~~The vertical sampling can be set to any multiple of 7.5 m, again depending on the science or validation need.~~ For the routine measurements contributing to NDACC over the period 1999-2015 and used for the present work, the standard settings have typically ranged between 5-min and 20-min for temporal sampling, and between 7.5 m and 75 m for the vertical sampling. Profiles routinely archived at NDACC are averaged over 2-hours, with an effective vertical resolution varying from 150-m to 3 km, decreasing with altitude. These temporal and vertical resolution settings yield a standard uncertainty of 7-14% throughout the profile. The system operates routinely at nighttime, but daytime measurements with reduced signal-to-noise

ratio are occasionally performed in special circumstances such as process studies, and aircraft or satellite validation. The total number of routine 2-hour ozone profiles used in this study and archived at NDACC for the period 2000-2015 is included in Table 1.

The TMF ozone lidar measurements have been regularly validated using simultaneous and co-located Electrochemical Concentration Cell (ECC) sonde measurements (Komhyr, 1969; Smit et al., 2007). In the troposphere the precision of the ozonesonde measurement is approximately 3-5% with accuracy of 5-10% below 30 km. TMF has ozonesonde launch capability since 2005 and 32 coincident profiles were obtained over the period 2005-2013. Results from the lidar and the ECC comparison are included in Figure 1.Figure1a shows the averaged relative difference between the lidar and ECC ozone number density profiles for the 32 cases. The lidar and sonde measurements are found to be in good agreement, with an average difference of 7% in the bulk of the troposphere and most of the values under 10% (Figure 1b), which is within the combined uncertainty computed from both the lidar and sonde measurements. Note that a non-negligible fraction of the differences is due to the different measurement geometry of the lidar and ozonesonde: 2-hour averaged, single location for lidar, and horizontally-drifting 1-second measurements for the ozonesonde usually rising at 5 $m \cdot s^{-1}$. Figure 1c reveals that the deviations do not present significant changes with time, which is an indicator of the system stability despite the multiple upgrades made over this time period. ~~In most cases, differences were within ±15% for the complete analyzed period. Note that a non-negligible fraction of the differences is due to geophysical variability. The measurement geometry of the lidar and ozonesonde are radically different: 2-hour averaged, single location for lidar, and horizontally-drifting instantaneous measurements for the ozonesonde.~~

2.2. Surface ozone measurements

Continuous surface ozone measurements have been performed at TMF since 2013 using the UV photometry technique (Huntzicker et al., 1979) with a UV photometric ozone analyzer (Model 49i from Thermo Fisher Scientific, US). The operation principle is based on the absorption of UV light at 254 nm by the ozone molecules (Shina et al., 2014). The instrument collects in-situ air samples at 2 meter above ground taken from an undisturbed forested environment adjacent to the lidar building. It provides ozone mixing ratio values at 1-minute time intervals with a lower

detection limit of 1 ppbv. Uncertainty has been reported to be below 6% in previous studies (Shina et al., 2014).

3. Results

3.1. Surface ozone variability

Figure 2a shows the surface ozone seasonal cycle at TMF and nearby stations from the California Air Resources Board (ARB) air quality network for the period 2013-2015. The seasonal cycle at TMF comprises a maximum in spring and summer and a minimum in winter, consistent with the ARB stations shown, as well as other stations in the US West Coast (e.g. Schnell et al., 2015). Nonetheless, the seasonal cycle obtained at TMF from the hourly samples (left plot) presents larger ozone values and lower variability throughout the year compared to the other ARB stations, all of which are at lower altitudes. The mean surface value for the complete period at TMF is 55 ppbv, whereas the seasonal values are 57, 57, 52 and 45 ppbv in spring (March-April-May), summer (June-July-August), fall (September-October-November) and winter (December-January-February) respectively. These values are in good agreement with those obtained from surface measurements at high elevation sites in the Northern Hemisphere and reported in the review by Cooper et al., (2014). When using the 8hMDA (8-h maximum daily average, right plot), larger seasonal-cycle amplitudes occur, especially at stations affected by anthropogenic pollution such as Crestline or San Bernardino. These polluted stations present larger values in summer than those recorded at high-elevation remote stations like Joshua Tree or TMF. The mean 8hMDA at TMF is 58 ppbv and the seasonal averages are 62, 66, 57 and 49 for spring, summer, fall and winter respectively. The observed low seasonal variability is typical of high-elevation remote sites with low urban influence (Brodin et al., 2010). A similar behavior can be observed at the Phelan, Joshua Tree or the Mojave National Preserve stations, all sites being at high elevation with low or negligible urban influence. In Figure 2a a secondary minimum is observed at TMF and most of the ARB nearby stations in July-August, followed by a secondary maximum in fall.

In Figure 2a a clear combined effect of the altitude and proximity to anthropogenic pollution sources on the ozone levels is observed. In general, higher ozone levels and lower variability are observed at higher altitudes. The lowest altitude Pico Rivera instrument measures the lowest ozone levels, and the highest-altitude TMF instrument measures the highest ozone levels throughout the year when considering the hourly sampled dataset. A mean difference of ~30 ppbv is observed for a 2-km altitude difference. The magnitude of this positive ozone vertical gradient depends on the distance from anthropogenic pollution sources. The effect of pollution is clearer on the 8hMDA data, where high-elevation stations, yet more likely to be affected by pollution such as Crestline or Victorville, present a larger seasonal cycle amplitude associated with lower ozone levels in winter and higher levels in summer. A similar impact of the interplay between urban influence and high-elevation was previously reported by Brodin et al., (2010).

The difference between the seasonal cycle retrieved from the 1-hour averaged data and the 8hMDA can be easily explained from the differences in the daily cycles at the different stations. The mean surface ozone diurnal cycle at TMF and nearby ARB stations is shown in Figure 2b for the four seasons. Minimum values are observed at nighttime, whereas maxima appear in late afternoon. As for the seasonal cycle, the daily cycle at TMF, Joshua Tree, Mojave National Preserve and Phelan stations exhibit low variability compared to the other stations located at lower altitude and more affected by urban pollution. On average, daily values are larger at high-elevation remote sites such as TMF or Joshua Tree. However, the afternoon maximum is larger at polluted stations such as Crestline, especially in the summer season. In addition, the maximum at TMF and the ARB stations of Joshua Tree and Mojave National Preserve occurs later than at the other stations. The difference in timing is likely due to the different chemical species involved in the ozone formation and depletion processes due to the low influence of anthropogenic pollution (Brodin et al., 2010; Gallardo et al., 2000; Naja et al., 2003). In winter, a minimum is observed at TMF in the afternoon instead of the maximum observed at the other stations. This difference in diurnal pattern has been observed at other remote or high-elevation sites and has been attributed to the shorter day length and the lack of ozone precursors compared to urban sites. The resulting daytime photochemical ozone formation is insufficient to produce an ozone diurnal variation maximizing in the afternoon (Brodin et al., 2010; Gallardo et al., 2000; Naja et al., 2003; Oltmans and Komhyr, 1986; Pochanart et al., 1999; Tsutsumi and Matsueda, 2000).

3.2.Tropospheric ozone variability

The red curve in Figure 3a (left plot) shows the average ~~tropospheric~~ ozone profile in the troposphere and the UTLS region obtained by the TMF lidar for the period 2000-2015. The cyan horizontal bars show the corresponding standard deviation at 1-km interval. The red dot at the bottom of the profile shows the 2013-2015 mean surface ozone obtained from the data acquired simultaneously to the lidar measurements. The lidar system provides information from approximately 1.3 km (from 200 meters since 2013) above the surface up to 25 km, covering the whole troposphere and the lower stratosphere. The average mixing ratio value in the mid-troposphere is 55 ppbv. Above 8 km, the ozone mixing ratio increases, reaching values above 1000 ppbv at 16 km.

The seasonally averaged profiles are shown in Figure 3b. These averages represent larger values in spring and summer in the troposphere, whereas in the stratosphere maximum values occur in winter and spring. Within the troposphere, below 9 km, the seasonally-averaged profiles show average values of 62, 60, 51 and 50 ppbv in spring, summer, fall and winter respectively. These values are in good agreement with the average ozone concentrations (50-70 ppbv) obtained in previous studies (Thompson et al., 2007; Zhang et al., 2010) above the western U.S. In the altitude range 9-16 km (UTLS) a much larger variability in ozone is observed, as indicated by the large standard deviation (left plot) and the differences between the seasonally-averaged profiles (right plot). This large variability results from the horizontal and vertical displacement of the tropopause above the site, causing the lidar to sound either the ozone-rich lowermost stratosphere or the ozone-poor sub-tropical upper troposphere for a given altitude.

The 2D color contours of Figure 4 show the composite (2000-2015) monthly mean ozone climatology measured by lidar (main panel, 4-20 km). A similar 2D color contour representation was used just below the main panel to represent the composite (2013-2015) monthly mean surface ozone. The climatological tropopause height at TMF is also included in the main panel (blue dotted line), with mean values ranging between 12 and 15 km. As discussed previously in this paper, the tropopause height variability is the main cause of the larger standard deviation observed in Figure 3a in this region. Between the surface and 9 km, a very consistent seasonal pattern occurs, with maximum values in April-May and minimum values in winter. The spring-summer maximum in the free-troposphere has been consistently observed at other stations in

Europe and North America and is commonly attributed to photochemical production (Law et al., 2000; Petetin et al., 2015; Zbinden et al., 2006). The maximum values in the Western US are also usually related to the influence of Asian emissions reaching the US West Coast (Jaffe et al., 2003; Parrish et al., 2004; Cooper et al., 2005; Neuman et al., 2012; Zbinden et al., 2013). Above 9 km, the seasonal maximum occurs earlier (i.e. in March and April between 10 and 12 km and February and March at higher altitudes) consistent with the transition towards a dynamically-driven lower-stratospheric regime. At these altitudes, the ozone minimum is also displaced earlier in the year (August-October), which is consistent with the findings of Rao et al. (2003) above Europe.

The TMF surface and lidar data are found to be very consistent, both in terms of seasonal cycle phase and amplitude, and in term of absolute mixing ratio values. The mean value obtained from the lidar measurements in the troposphere is very similar to the mean value obtained from the surface measurements (around 55 ppbv). This consistency points out that the TMF surface measurements are representative of the lower part of the free troposphere (i.e., below 7 km), at least during the nighttime lidar measurements. This is mostly due to the fact that the station is not affected by the boundary layer during most of the time because of its high-elevation. Additional daytime lidar measurements will be performed in 2016 to assess whether such consistency also exists at other times of the day, especially in the afternoon.

~~The consistency between the lidar and the surface data was found not only for the seasonal cycle obtained from the monthly averaged values, but also for the complete time series. The degree of correlation between the lidar measurements at the lowest point and the surface measurements was investigated. As mentioned before, the lidar cannot measure all the way down to the surface. The first valid measurement occurs at around 3.5-4 km depending on the time period. Therefore, the layer from 4 to 6 km is considered as the lower lidar layer. A correlation coefficient of R=0.34 was found between the lidar data in the layer from 4 to 6 km and the surface data. The correlation increases (R=0.44) if we consider a 3-hour time lag between the 4-6 km layer and the surface. After removing outliers corresponding to ozone values higher (or lower) than the average plus (minus) one standard deviation either at the surface or at 4-6 km, the correlation increases up to 0.69 for the simultaneous data and up to 0.79 for the 3-hour time-shift.~~

3.3.Interannual variability and trends

The 2000-2015 time-series of the deseasonalized ozone mixing ratio is shown in Figure 5. Anomalies, expressed in percent, resulted from subtracting the climatological ozone monthly mean profiles computed for the period 2000-2015 to the measured lidar profiles. Large ozone variability with time is clearly observed, highlighting the difficulty in identifying trends and patterns. No clear mode of interannual variability is observed for the analyzed period here. However, positive anomalies seem to predominate throughout the troposphere during the period 2003-2007, especially below 7 km. On average, ozone mixing ratio values in the lower troposphere were 5 ppbv larger in 2003-2007 than during the entire period 2000-2015.

Following a procedure similar to that described in Cooper et al. (2012), a trend analysis was performed at different altitude levels (Tables 2 and 3 and Figure 6). Figure 6 shows the time series of the median, 95^{th} and 5^{th} percentile values, obtained every year between 2000 and 2015 for different layers and different seasons using the lidar profiles measured at TMF. In order to obtain the trends, linear fits (shown in Figure 6) of the median, 95^{th} and 5^{th} percentiles were performed independently using the least squares method. The ozone rate of change in ppbv.year^{-1} was determined from the slope of the linear fit. To assess the significance of the trends, the F-statistic test was used, with the p-Value as an indicator of the statistical significance. P-Values lower than 0.05 (0.10), indicate statistically significant trends, with a confidence level larger than 95% (90%).

The calculated trends ~~were found to~~ depend on altitude and season. Table 1. Number of measurements, by month and years, performed at TMF with the tropospheric ozone DIAL system. N/A indicates data not available at the time of the study

	Jan	Feb	Mar	Apr	May	Jun	Jul	Aug	Sep	Oct	Nov	Dec	Total
2000	4	2	6	4	11	12	7	10	8	1	0	0	65
2001	1	11	17	2	9	13	12	15	15	17	8	10	130
2002	6	10	6	4	0	10	11	1	6	16	12	11	93
2003	11	9	15	12	10	13	5	7	9	14	7	5	117
2004	9	8	15	14	12	6	12	13	11	10	9	11	130
2005	4	6	13	8	12	16	9	2	7	2	11	9	99
2006	11	9	6	8	14	5	2	12	12	20	6	1	106
2007	0	0	4	9	11	7	8	10	8	26	10	8	101
2008	7	11	8	13	9	4	11	10	6	11	4	6	100
2009	14	11	7	5	7	8	4	10	4	17	1	3	91
2010	0	0	3	8	0	7	4	1	4	5	9	3	44
2011	2	6	4	7	7	11	10	12	7	8	8	8	90

2012	0	9	9	1	10	13	3	2	5	8	4	5	69
2013	6	3	5	10	8	7	5	7	0	0	0	0	51
2014	9	2	5	10	13	16	15	11	15	15	14	6	131
2015	9	15	12	18	3	14	12	N/A	N/A	N/A	N/A	N/A	83
Total	93	112	135	133	136	162	130	123	117	170	103	86	1500

Table 2 contains the ozone rate change expressed in ppbv.year^{-1} (and %.year^{-1}) for the different layers and seasons for the median, 5th and 95th percentiles. The corresponding standard errors and p-Values are included in Table 3. Statistically significant trends at 95% and 90% confidence levels are marked in bold font and underlined respectively. The layer corresponding to the upper troposphere (7-10 km) shows a statistically significant ozone increase of 0.31±0.15 ppbv.year^{-1} (0.57±0.28 %·year^{-1},p =0.06 for the median values and 0.55±0.30 ppbv.year^{-1} (0.54±0.29 %.year^{-1},p =0.09 for the 95th percentile, indicating that both the background and the high intensity ozone events levels were increasing (Cooper et al., 2012, 2014). Cooper et al. (2012) reported a similar increase in the free troposphere and in the western US for the period 1990-2010 for both the median and 95th percentiles.

Analyzing each season separately, a significant positive trend occurs in the upper troposphere (7-10 km) for both spring and summer, with an ozone increasing rate of 0.71±0.25 and 0.58±0.28 ppbv.year^{-1} respectively (or 1.10±0.39% and 0.98±0.47%·year^{-1}, p=0.01 and p=0.05, and an ozone decrease of -0.43±0.18 ppbv.year^{-1} (-0.87±0.34 %·year^{-1}, p=0.03) during winter. Statistically significant negative trends were also found in the lower troposphere (4-7 km) during winter for the median and 5th percentile values with an ozone decrease of -0.36±0.16 ppbv.year^{-1} and -0.59±0.18 ppbv.year^{-1} respectively (-0.72±0.32%·year^{-1}, p=0.04, and -1.53±0.47%·year^{-1}, p=0.0004, respectively) (Table 2). Trends near the tropopause (12-16 km) are not significant, whereas a significant negative trend of -8.8±4.5 ppbv.year^{-1} (-1.39±0.71%·year^{-1},

p=0.07) for the median and -5.8±2.9 ppbv.year^{-1} (-1.26±0.63%·year^{-1}, p=0.07) for the 5th percentile in fall was calculated in the lower stratosphere (17-19 km).

The positive trend at TMF in spring for the median values is larger than the trend obtained by Cooper et al. (2012) for the free troposphere in 1995-2011 (0.41±0.27 ppbv.year^{-1}), and even larger than the trend obtained by Lin et al. (2015b) using model data (0.36±0.18 ppbv.year^{-1} during 1995-2014). This disagreement could be due to differences in sampling, as concluded in Lin et al. (2015b). Nonetheless, Figure 6 shows larger ozone median (and 5th and 95th percentile) values at 7-10 km in 2013-2015 than in preceding years. A lower ozone increasing rate in 2000-2012 above TMF (0.56 ppbv.year^{-1}) suggests that the ozone rate of change has increased in the last years, but a more comprehensive study with regional coverage would be necessary to confirm the significance of this change. Regarding winter season, a positive trend was obtained on a regional scale in Cooper et al., (2012), but certain sites in the western U.S. showed a negative trend, even though not statistically significant. Analyzing the period 2000-2010 as in Cooper et al., (2012), we still observe a negative trend at TMF (-0. 07 ppbv.year^{-1}), but it is not statistically significant for this shorter period (p=0.83).

The springtime positive trend estimates reported in the Western US oppose ozone decrease in the Eastern part. These results indicate that the two-decade-long efforts to implement regulations to control air quality and anthropogenic emissions in the U.S. have led to a clear decrease in ozone levels in the Eastern U.S., but not in the Western U.S. (e.g. Copper et al., 2012; 2014). This different regional behavior has been attributed to the inflow of elevated ozone, mainly from East Asia, and to the increasing contribution of stratospheric intrusions (Cooper et al., 2010; Jacob et al., 1999; Parrish et al., 2009; Reidmiller et al., 2009; Lin et al., 2012a; 2015a: Lefohn et al., 2011; 2012). But again, differences in sampling can impact significantly the interpretation of our trend estimates. As pointed out by Lin et al. (2015b), further coordination efforts at both global and regional scales are necessary in order to reduce biases introduced by inhomogeneity in sampling.

3.4.Characterization of the air masses sounded by the TMF tropospheric ozone lidar

In an attempt to characterize the air parcels sounded by lidar above TMF based on their travel history and analyze the influence of the different source regions on the ozone profiles, 12-day

backward trajectories ending at TMF between 5 and 14 km altitude were computed using the HYSPLIT4 model (Draxler and Rolph, 2003), http://www.arl.noaa.gov/ready/hysplit4.html). The NCAR/NCEP Reanalysis Pressure level data were used as meteorological input (Kalnay and Kanamitsu, 1996) in HYSPLIT4. These data, available since 1948, provide 4-times-daily meteorological information at 17 pressure levels between the 1000 and 10 hPa and 2.5x2.5 degrees horizontal resolution. Several studies (Harris et al., 2005; Stohl, 1998) provided a wide range of uncertainty estimates along the trajectories. The more recent study by Engström and Magnusson, (2009) indicates that the uncertainty of the trajectories is within 354-400 km before 4 days and 600 km after.

Our trajectory analysis comprises two steps. First, the 12-day backward trajectories computed by HYSPLIT and ending at different altitude levels were grouped using the HYSPLIT clustering tool (Draxler et al., 2009) in order to identify the most significant paths followed by the air masses arriving over the station. Based on the results of this preliminary analysis, five main regions were identified: the stratosphere, the Asian boundary layer (ABL), the free-troposphere above Asia (AFT), Central America, and the Pacific Ocean. Once these geographical areas were identified, we performed a classification of the air parcels according to the criteria described next.

An air parcel was classified as "Stratospheric" if the 12-day backward trajectory intercepted the tropopause and resided at least 12 hours above the local tropopause. The tropopause height information comes from the global tropopause height data derived once a day by the NOAA Physical Sciences Division (http://www.esrl.noaa.gov/psd) from the same NCAR/NCEP Reanalysis database used as input to HYSPLIT4. Computations are based on the World Meteorological Organization (WMO, 1957) definition, that is, the lowest height at which the temperature lapse rate becomes lower than 2 $K \cdot km^{-1}$, provided that along 2 km above this height the average lapse is also lower than 2 $K \cdot km^{-1}$. In addition, the NOAA computations do not allow tropopause heights at pressure levels larger than 450 hPa and smaller than 85 hPa. The residence time of the air masses in the stratosphere was selected based on a sensitivity test, which indicated that time residences larger than 6 hours already show a significant signature of the stratospheric ozone in the ozone profiles within the troposphere. However, to avoid an overestimation of the stratospheric cases a 12 hours residence time was found to be more appropriate for our analysis.

Next, the air parcels that were not classified as "Stratosphere" were then classified as "Central America" for trajectories comprising a minimum residence time of 4 days within the area labelled "Central America" in Figure 7. According to the sensitivity test, a 4 days residence time period is long enough to avoid the influence of additional source regions and short enough to avoid an underestimation of the "Central America" cases.

The air parcels not classified as "Stratosphere", or "Central America" were then classified as Asian if they comprised a minimum residence time of 6 hours within the area labelled as "Asia" in Figure 7. The Asian trajectories are subdivided in "Asian Boundary Layer" (ABL) if they come from an altitude below 3 km and "Asian Free-troposphere" (AFT) if they come from altitudes above 3 km. According to the sensitivity test, a residence time of 6 hours is enough to clearly identify the signature of Asian emissions on the ozone profiles observed at TMF.

The air parcels not classified in any of the previous categories were classified as "Pacific Ocean" if a minimum residence time of 276 hours (11.5 days) within the area labelled "Pacific" in Figure 7 was reached. A residence time of 276 hours guarantees that no influence from additional sources affects the air masses reaching TMF and the "Pacific" region can be considered as a background region.

Trajectories that did not match any of the previous categories were grouped as "residual trajectories" (RT). They will be considered for statistical purposes, but not for the analysis of the ozone mixing ratio values.

The classification of the air parcels took place sequentially, which means that each category is exclusive of the others. The classification was made for each of the four seasons separately in order to account for the seasonal changes in synoptic circulation. Examples of the corresponding classified back-trajectories are shown in Figure 8. The number and frequency of occurrences of each air parcel category for all seasons is compiled in Table 4. A monthly distribution of these occurrences is shown in Figure 9. With the selection criteria we have set, air masses are predominantly associated to the "AFT" region below 11 km, ranging between 32 and 42% from 5 to 11 k with maximum number of cases in spring. A very low number of parcels classified as "ABL" are found (between 0 and 9%). Increasing influence of the stratosphere is observed at upper levels, with values increasing from 5% at 5 km to 80% at 14 km. Higher influence is

observed during winter and spring, which agrees well with previous studies in the Western US (Sprenger, 2003; Stohl, 2003). A statistically significant Central American influence was identified in summer with a frequency of occurrence varying between 120% and 3%, decreasing with altitude. The Central America influence coincides with the establishment of the North American Monsoon circulation from July to September and which affects Central America and the Southern US.

Composite ozone profiles and statistical parameters were estimated for each category of air parcel and for altitudes between 5 and 14 km at 1-km altitude intervals. Figure 10 shows the ozone mixing ratio mean (open circles), median (red bars), 25^{th} and 75^{th} percentiles (blue bars) at 9 km altitude for each of the identified categories and season. The number of occurrences for each category is mentioned between parentheses. The ozone statistics obtained when a low number of occurrences was found should be ignored (e.g., Central America except for Summer, or ABL for Winter and Fall). Figure 11a shows, for each season, the composite ozone profiles constructed from the ozone mixing ratio median values found for a particular category at a given altitude. The same profiles but focused on the troposphere (5-10 km) are shown in Figure 11b. In order to keep the most statistically significant results, composite values computed using less than 5% of the total number of samples for a given season were not plotted, leaving out certain sections of the composite profiles.

Not surprisingly, the analysis reveals that the largest ozone mixing ratio values were mostly observed when the air masses were classified as "stratospheric" regardless of the season (median values between 17 and 35 ppbv larger than for the Pacific Ocean at 9 km). In spring and winter, the influence of the stratosphere goes down to 5 km, with ozone values ranging from 3 to 13 ppbv larger than for the Pacific category below 9 km. For this category, large ozone variability was found, as indicated by the 25^{th} and 75^{th} percentiles in Figure 10. As altitude increases, the influence of the stratosphere is more important, exceeding 40% above 12 km, resulting in higher ozone mixing ratio values (red curves in Figure 11).

Conversely, low ozone mixing ratio values (40-61 ppbv below 9 km) were consistently associated with the air parcels classified as "Pacific Ocean" (cyan curves). This region can be considered as a source of 'background ozone', since no anthropogenic source is expected to affect the local ozone budget.

Higher ozone content (from 2 to 13 ppbv higher than for the Pacific region) is systematically found for air parcels classified as "AFT". Values are especially larger in summer, when differences of at least 8 ppbv with the Pacific region are found for altitudes between 5 and 13 km. In general, the number of occurrences for air parcels classified as "ABL" remains very small to provide any meaningful interpretation. Nonetheless, values in the lower part of the troposphere during spring and winter, when the number of occurrences is higher, are similar to those observed for the AFT. The occurrence of the Asian air masses is mostly observed in spring (Figures 9 and 10), and ozone associated to Asian emissions has been frequently detected in the Western US during this season in previous studies (e.g. Cooper et al., 2005; Zhang et al., 2008; Lin et al., 2012). Even though less frequent, our results indicate that Asian pollution episodes observed during summer are associated to larger ozone values than in spring. These larger values are due to more active photochemical ozone production observed over China in summer (Verstraeten et al., 2015), associated to larger ozone values than those in spring. The influence of the air parcels classified as Central America is mainly observed during summer, with ozone median values 5-28 ppbv larger than those observed for the Pacific region between 5 and 9 km (yellow curve in Figure 11). Ozone mean values of 72 ppbv were found at 9 km altitude for the 74 air parcels classified as "Central America" (Figure 10). The corresponding values for the 115 air parcels classified as "Pacific Ocean" are about 52 ppbv, which is 20 ppbv lower. The larger ozone values associated to the "Central America" category possibly points out to the lightning-induced enhancement of ozone within the more frequent occurrence of thunderstorms during the North American summer monsoon. Previous studies (Cooper et al., 2009), have observed enhanced ozone values associated with the North American Monsoon, mainly due to ozone production associated with lightning (Choi et al., 2009; Cooper et al., 2009). However, this feature was observed in the Eastern U.S. Because of the synoptic conditions during the monsoon, the Western U.S. is not as much influenced and no significant regional ozone increase was reported (Barth et al., 2012; Cooper et al., 2009). Nevertheless, Cooper et al., (2009) reported higher modeled lightning-induced NO_x concentrations at TMF than at other western locations, which would be consistent with our findings. Further investigation, including a detailed history of the meteorological conditions along the trajectories and chemistry transport model data, is needed to confirm this correlation. Additional sources, such as ozone transport from Central America or even mixing with different sources (e.g. the stratosphere) should also be considered.

3.5.The influence of tropopause folds on the TMF tropospheric ozone record

In the previous section, a large variability in the composite ozone content was found for the air parcels classified as "Stratospheric". In the current section, we provide at least one clear explanation for this large variability. Tropopause folds are found primarily in the vicinity of the subtropical jets, in the 20º-50º latitude range. They typically consist of three-dimensional folds of the virtual surface separating air masses of tropospheric characteristics (weakly stratified, moist, low ozone concentration, etc.) and those of stratospheric characteristics (highly stratified, dry, high ozone concentration, etc.). Tropopause folds can result in the transport of large amounts of stratospheric ozone into the troposphere, reaching in some cases the planetary boundary layer and enhancing ozone amounts even at the surface (Chung and Dann, 1985; Langford et al., 2012; Lefohn et al., 2012; Lin et al., 2012a). They are considered one of the main mechanisms of stratosphere-to-troposphere exchange and have been widely studied in the past (e.g. Bonasoni and Evangelisti, 2000; Danielsen and Mohnen, 1977; Lefohn et al., 2011; Vaughan et al., 1994; Yates et al., 2013). Due to the location of TMF, the upper troposphere above the site is frequently impacted by tropopause folds.

Double tropopauses are usually expected to result from tropopause folds in the layer between the two identified tropopauses. Therefore, a common method used in the literature to identify tropopause folds is to detect the presence of double tropopauses based on temperature profiles (e.g. Chen et al., 2011). The MERRA (Modern-Era Retrospective analysis for Research and Applications, Rienecker et al., 2011) reanalysis data (1-km vertical resolution, 1 x 1.25 degrees horizontal resolution) were used in this study to identify the presence of double tropopauses above the station. A comparison between the MERRA temperature profiles and the temperature profiles measured by the radiosondes launched at TMF was performed in order to evaluate the performance of MERRA above TMF. The comparison (not shown) reveals excellent agreement, with average relative differences of 2% or less from the surface up to 25 km. The heights of double tropopauses were computed following a methodology similar to that proposed in Chen et al., (2011) and Randel et al., (2007). The first (lower) tropopause is identified according to the WMO definition, as explained earlier. A second (upper) tropopause is identified above the WMO tropopause if the temperature lapse rate increases over 3 $K \cdot km^{-1}$ within at least 1 km, and its height is determined once again by the WMO criterion.

Using this methodology, we found that 27% of the TMF tropospheric ozone lidar profiles were measured in the presence of double tropopauses. This high frequency of double tropopause occurrences was expected considering the latitude of TMF, i.e., near the subtropical jet, where frequent tropopause folds occur. Figure 12 shows the number of cases with double tropopauses above TMF distributed per months, with the number of days with double tropopause being normalized to the total number of measurements every month (compiled in Table 1). As we can see, the presence of double tropopauses was especially frequent during winter and spring, which coincides with the higher frequency of stratospheric air masses arriving at TMF estimated by the backward trajectories analysis (Figure 9) and is in agreement with previous studies (Randel et al., 2007). The altitude of detected single tropopauses is found around 13 km in winter and spring, and 16-17 km in summer and fall (Figure 13a-d). When a double tropopause is identified, the altitude of the lower tropopause ranges between 8 and 15 km, with the distribution peak centered around 12-13 km (Figure 13e-h), and the second tropopause is detected typically around 17-18 km (Figure 13i-l).

Figure 14a shows an example of an ozone profile measured on January 8, 2013, when a double tropopause was detected above TMF. The average of all tropospheric ozone lidar profiles measured in winter in cases of single tropopause is plot as reference. In Figure 14b, the average of all tropospheric ozone lidar profiles measured in winter (blue curves) and spring (red curves) in the presence of a double tropopause (solid curves), and in the presence of a single tropopause (dashed curves) are included. The right panel (Figure 14c) is simply a lower tropospheric-zoomed version of the middle panel (Figure 14b). Only winter and spring are shown because they are the seasons most affected by double tropopause cases as previously stated. In the presence of double tropopauses a clear dual vertical structure in ozone is observed. For the specific case on January 8, 2013 (Figure 14a), the lower tropopause was located at 9 km and stratospheric air reached down to approximately 6 km, considerably increasing the ozone content in the troposphere. On the other hand, ozone values were lower than the winter average in the lower stratosphere (11-19 km). In the case of the average profiles (Figure 14b) the dual vertical structure presents higher ozone values between 12 and 14 km and lower mixing ratio values between 14 and 18 km. The dual ozone structure observed by lidar coincides with the expected location of the fold, and consists of systematically higher-than-average mixing ratios in the lower half of the fold (12-14 km), and lower-than-average mixing ratios in the upper half of the fold

(14-18 km). This dual structure is consistent with the expected origin of the air masses within a tropopause fold. Stratospheric air, richer in ozone, is measured within the lower half of the fold, while tropospheric ozone-poor air is measured within the upper half of the fold.

In the case of deep stratospheric intrusions, ozone-rich stratospheric air masses embedded in the lower half of the fold can reach lower altitudes, and occasionally the planetary boundary layer mixing down to the surface (Chung and Dann, 1985; Langford et al., 2012, 2015; Lefohn et al., 2012; Lin et al., 2012a), leading to an ozone increase in the lower troposphere (Figure 14b). In our case, the mean increase is around 2 ppbv below 6 km for both spring and winter. This increase is consistent with previous reports of the importance of the stratosphere as an ozone source in the lower troposphere (Cooper and Stohl, 2005; Langford et al., 2012; Lefohn et al., 2011; Trickl et al., 2011), with a 25 to 50% contribution to the tropospheric budget (Davies and Schuepbach, 1994; Ladstätter-Weißenmayer et al., 2004; Roelofs and Lelieveld, 1997; Stevenson et al., 2006)

~~4. Discussion~~

~~The present study allowed the characterization of the full tropospheric ozone profile from the ground to the stratosphere, and is particularly valuable in the context of a notoriously sparse horizontal coverage for this type of vertically resolved measurements in a region affected by transboundary ozone inflow and stratospheric intrusions.~~

~~The combined analysis of the surface measurements and the simultaneous lidar profiles reveals high consistency between the ozone at the surface and in the free troposphere. This consistency may point out the fact that the TMF surface measurements are representative of the lower part of the free troposphere (i.e., below 7 km), at least during the nighttime lidar measurements. Additional daytime lidar measurements will be performed in 2016 to assess whether such consistency also exists at other times of the day, especially in the afternoon.~~

~~The analysis of the long-term lidar time-series (16 years covered) shows no significant signatures of interannual variability, as previously discussed. More importantly, no obvious signature of ENSO or the QBO could be identified, which is inconsistent with the recent findings of Lin et al., (2015) or Neu et al., (2014), who have linked tropospheric ozone variability in the Northern Hemisphere to El Niño/ La Niña events, and the QBO, through the variations of~~

stratospheric/tropospheric ozone fluxes. However, this inconsistency might not be so surprising if we take into account the obvious difference in measurement sampling (one single location in the Western U.S. as opposed to global observations).

Nevertheless, our analysis reveals statistically-significant trends for selected seasons and altitudes. Specifically, a positive trend of 0.31 ppbv.year^{-1} (ozone annual median) was found in the upper troposphere (7-10 km). This positive trend is more pronounced in spring and summer (0.71 and 0.58 ppbv.year^{-1} respectively), while a negative trend (-0.43 ppbv.year^{-1}) was found in winter. The positive trend obtained here in spring for the median values is larger than the trend obtained by Cooper et al. (2012) for the free troposphere in 1995-2011 (0.41 ppbv.year^{-1}), and even larger than the trend obtained by Lin et al. (2015b) using model data (0.37 ppbv.year^{-1} during 1995-2012). This disagreement could be due to differences in sampling, as concluded in Lin et al. (2015b). Nonetheless, Figure 6 shows larger ozone median (and 5th and 95th percentile) values at 7-10 km in 2013-2015 than in preceding years, with this period not being included in the previous studies. A lower ozone increasing rate in 2000-2012 above TMF (0.43 ppbv.year^{-1}) suggests that that the ozone rate of change has increased in the last years, but a more comprehensive study with regional coverage would be necessary to confirm this change. Regarding winter season, a positive trend was obtained on a regional scale in Cooper et al., (2012), but certain sites in the western U.S. showed a negative trend, as in our case. This negative trend indicates a decrease in the background ozone values. During winter months, a smaller influence of transboundary ozone transport is expected at low altitudes above TMF and the decrease in background ozone during these months could be associated with the decrease in domestic anthropogenic emissions.

The springtime positive trend estimates reported in the Western US oppose ozone decrease in the Eastern part. These results indicate that the two-decade-long efforts to implement regulations to control air quality and anthropogenic emissions in the U.S. have led to a clear decrease in ozone levels in the Eastern U.S., but not in the Western U.S. (e.g. Copper et al., 2012; 2014). This different regional behavior has been attributed to the inflow of elevated ozone, mainly from East Asia, and to the increasing contribution of stratospheric intrusions (Cooper et al., 2010; Jacob et al., 1999; Parrish et al., 2009; Reidmiller et al., 2009). But again, differences in sampling can impact significantly the interpretation of our trend estimates. As pointed out by

Lin et al. (2015b), further coordination efforts at both global and regional scales are necessary in order to reduce biases introduced by inhomogeneity in sampling. As part of these efforts, an extended analysis based on the origin of the air masses sampled by the TMF lidar is under way, with the ultimate objective to filter synoptic noise out, and better quantify the ENSO and QBO signals and the residual trends. As a prerequisite to such study, a preliminary characterization of the air masses sounded by the TMF lidar was performed and presented here.

Backward trajectories analysis reveals that, not surprisingly, parcels identified as "stratosphere" contain the highest ozone mixing ratios, and parcels classified as "Pacific Ocean" contain the lowest ozone concentrations, which can be considered as 'background conditions'. Despite influence of Asian pollution in the ozone levels in the Western US has been detected in previous studies (e.g. Zhang et al., 2008; Lin et al., 2012; Langford et al., 2015), no outstanding signature from the Asian boundary layer could be identified due to the low number occurrences associated with this category in our case. Nevertheless, air parcels classified as "Asian free-troposphere" seemed to contain systematically more ozone than those classified as "Pacific Ocean", especially below 9 km. A refined classification, probably requiring the use of chemistry-transport models, is needed to assess whether the Asian boundary layer or the Asian free-troposphere have a detectable impact on the ozone content measured above TMF.

In summer, air masses coming from Central America were frequently detected. The ozone mixing ratio values measured in this case were clearly above the climatological mean, with values up to 15 ppbv larger than those associated with the Pacific Ocean region. Previous studies (Cooper et al., 2009), have observed enhanced ozone values associated with the North American Monsoon, mainly due to ozone production associated with lightning (Choi et al., 2009; Cooper et al., 2009). However, this feature was observed in the Eastern U.S. Because of the synoptic conditions during the monsoon, the Western U.S. is not as much influenced and no significant ozone increase was reported (Barth et al., 2012; Cooper et al., 2009). Nevertheless, Cooper et al., (2009) reported higher modeled lightning-induced NO_x concentrations at TMF than at other western locations, which would be consistent with our findings. Further investigation, including a detailed history of the meteorological conditions along the trajectories, is needed to confirm this correlation.

As part of the characterization of the TMF lidar-sampled air masses, the impact of double tropopauses was assessed. Between 2000 and 2015, the frequency of occurrence of double tropopauses above TMF was found to be around 27%. This high frequency, especially observed in winter and spring, was expected considering the latitude of TMF, i.e., near the subtropical jet, where frequent tropopause folds occur. More interestingly, a clear, dual vertical structure in ozone was observed in the presence of a double tropopause (Figure 14). The double tropopause is expected to result from a tropopause fold in the layer between the two identified tropopauses. The dual ozone structure observed by lidar coincides with the expected location of the fold, and consists of systematically higher-than-average mixing ratios in the lower half of the fold (12-14 km), and lower-than-average mixing ratios in the upper half of the fold (14-18 km). This dual structure is consistent with the expected origin of the air masses within a tropopause fold. Stratospheric air, richer in ozone, is measured within the lower half of the fold, while tropospheric ozone-poor air is measured within the upper half of the fold. In addition, statistically significant higher-than-average mixing ratios (+2 ppbv) are observed in the lower troposphere (4-10 km) in the presence of double tropopauses. This increase is consistent with previous reports of the importance of the stratosphere as an ozone source in the lower troposphere (Cooper and Stohl, 2005; Langford et al., 2012; Lefohn et al., 2011; Trickl et al., 2011), with a 25 to 50% contribution to the tropospheric budget (Davies and Schuepbach, 1994; Ladstätter-Weißenmayer et al., 2004; Roelofs and Lelieveld, 1997; Stevenson et al., 2006).

Further investigation is now underway, with the objective of better identifying all signatures of interannual variability and trends. This long-term variability investigation not only will include an air mass classification based on geographical area, but will also take into account the history of the air parcels in the context of nearby tropopause folds. Altogether, this air parcel characterization, used in conjunction with regional chemistry-climate or chemistry-transport model runs, should unveil signatures hidden in the current lidar record, and eventually shed new light on the origin of the reported past, current, and future tropospheric ozone trends over the Western U.S.

4. Concluding remarks

Combined ozone photometer surface measurements (2013-2015) and tropospheric ozone DIAL profiles (2000-2015) at the JPL-Table Mountain Facility were presented for the first time.

706 The high ozone values and low interannual and diurnal variability measured at the surface,
707 typical of high elevation remote sites with no influence of urban pollution, constitute a good
708 indicator of background ozone conditions over the Southwestern US.

709 The 16-year tropospheric ozone lidar time-series is one of the longest lidar records
710 available and is a valuable dataset for trend analysis in the Western US, where the number of
711 long-term observations with high vertical resolution in the troposphere is very scarce. A
712 statistically significant positive trend was observed in the upper troposphere, in agreement with
713 previous studies. This ozone increase points out to the influence of long-range transport and/or a
714 change in stratospheric influence, since ozone precursor emissions have been decreasing in the
715 US over the past two decades.

716 Influence of five main regions (stratosphere, Central America, Asian boundary layer,
717 Asian free troposphere and Pacific Ocean) on the ozone profiles sampled above TMF was
718 detected using 12-day backward trajectories. This trajectories analysis revealed the large
719 influence of the stratosphere, especially in the UTLS and the upper troposphere, leading to high
720 ozone values. The influence of the stratosphere reached down to 5 km in spring and winter, with
721 ozone values ranging from 3 to 13 ppbv larger than for the Pacific category, considered as a
722 background region. In summer, enhanced ozone values (5-28 ppbv larger than for the Pacific
723 region) were found in air parcels originating from Central America, probably due to the
724 enhanced thunderstorm activity during the North American Monsoon. Frequent air masses
725 coming from Asia were also observed, mainly in spring, associated to ozone values 2 to 13 ppbv
726 larger than those from the background region. Ozone vertical distribution above TMF is also
727 affected by the frequent occurrence of tropopause folds. A dual vertical structure in ozone within
728 the fold layer was clearly observed, characterized by above-average values in the bottom half of
729 the fold (12-14 km), and below-averaged values in the top half of the fold (14-18 km). Above-
730 average ozone values were also observed near the surface (+2 ppbv) on days with a tropopause
731 fold. The high frequency of tropopause folds observed above the site is not surprising given
732 Table Mountain's position in the vicinity of the subtropical jet. ~~A detailed and systematic~~
733 ~~analysis of the ozone vertical structure, and its variability in relation to the proximity of the~~
734 ~~subtropical jet is in preparation. This analysis, which will utilize a large amount of model data~~
735 ~~together with the lidar observations, should shed some light on a possible correlation between the~~

~~observed upper tropospheric ozone positive trends and the impact of the tropopause folds, either as a result of an increase in frequency of the stratospheric intrusions, or as a result of the mid-latitude stratospheric ozone recovery observed since the early 2000s (WMO, 2014).~~

ACKNOWLEDGEMENTS

The work described in this paper was carried out at the Jet Propulsion Laboratory, California Institute of Technology, under a Caltech Postdoctoral Fellowship sponsored by the NASA Tropospheric Chemistry Program. Support for the lidar, surface, and ozonesonde measurements was provided by the NASA Upper Atmosphere Research Program. The authors would like to thank M. Brewer, T. Grigsby, J. Howe, and members of the JPL Lidar Team who assisted in the collection of the data used here. The authors gratefully acknowledge the NOAA Air Resources Laboratory (ARL) for the provision of the HYSPLIT transport and dispersion model and/or READY website (http://www.ready.noaa.gov) and the NCEP/NCAR Reanalysis team for the data used in this publication. We would also like to thank Dr. Susan Strahan and the MERRA Reanalysis team for providing the data used in this study and to acknowledge the California Air Resources Board for providing the surface ozone data.

Copyright 2016. All rights reserved.

REFERENCES

Ambrose, J., Reidmiller, D. and Jaffe, D.: Causes of high O 3 in the lower free troposphere over the Pacific Northwest as observed at the Mt. Bachelor Observatory, Atmos. Environ., 2011.

Barth, M. C., Lee, J., Hodzic, A., Pfister, G., Skamarock, W. C., Worden, J., Wong, J. and Noone, D.: Thunderstorms and upper troposphere chemistry during the early stages of the 2006 North American Monsoon, Atmos. Chem. Phys., 12(22), 11003–11026, doi:10.5194/acp-12-11003-2012, 2012.

Bonasoni, P. and Evangelisti, F.: Stratospheric ozone intrusion episodes recorded at Mt. Cimone during the VOTALP project: case studies, Atmos. Environ, *34*(9), 1355-1365, 2000.

Brodin, M., Helmig, D. and Oltmans, S.: Seasonal ozone behavior along an elevation gradient in the Colorado Front Range Mountains, Atmos. Environ., 44(39), 5305–5315, doi:10.1016/j.atmosenv.2010.06.033, 2010.

Brown-Steiner, B. and Hess, P.: Asian influence on surface ozone in the United States: A comparison of chemistry, seasonality, and transport mechanisms, J. Geophys. Res., 116(17), 1–13, doi:10.1029/2011JD015846, 2011.

Bufton, J. L., Stewart, R. W. and Weng, C.: Remote measurement of tropospheric ozone., Appl. Opt., 18(20), 3363–4, doi:10.1364/AO.18.003363, 1979.

Choi, Y., Kim, J., Eldering, A., Osterman, G., Yung, Y. L., Gu, Y. and Liou, K. N.: Lightning and anthropogenic NOx sources over the United States and the western North Atlantic Ocean: Impact on OLR and radiative effects, Geophys. Res. Lett., 36(17), L17806, doi:10.1029/2009GL039381, 2009.

Chung, Y. and Dann, T.: Observations of stratospheric ozone at the ground level in Regina, Canada, Atmos. Environ., *19*(1), 157-162, 1985.

Cooper, O. R., Forster, C., Parrish, D., Trainer, M., Dunlea, E., Ryerson, T., Hübler, G., Fehsenfeld, F., Nicks, D., Holloway, J., de Gouw, J., Warneke, C., Roberts, J. M., Flocke, F. and Moody, J.: A case study of transpacific warm conveyor belt transport: Influence of merging airstreams on trace gas import to North America, J. Geophys. Res., 109(D23), n/a–n/a, doi:10.1029/2003JD003624, 2004.

Cooper, O. R., Stohl, A., Eckhardt, S., Parrish, D. D., Oltmans, S. J., Johnson, B. J., Nédélec P., Schmidlin, F. J., Newchurch, M. J., Kondo, Y., and Kita, K.: A springtime comparison of tropospheric ozone and transport pathways on the east and west coasts of the United States, J. Geophys. Res., 110, D05S90, doi: 10.1029/2004JD005183, 2005.

Cooper, O. R., Eckhardt, S., Crawford, J. H., Brown, C. C., Cohen, R. C., Bertram, T. H., Wooldridge, P., Perring, A., Brune, W. H., Ren, X., Brunner, D. and Baughcum, S. L.: Summertime buildup and decay of lightning NO_x and aged thunderstorm outflow above North America, J. Geophys. Res., 114(D1), D01101, doi:10.1029/2008JD010293, 2009.

Cooper, O. R., Parrish, D. D., Stohl, A., Trainer, M., Nédélec, P., Thouret, V., Cammas, J. P., Oltmans, S. J., Johnson, B. J., Tarasick, D., Leblanc, T., McDermid, I. S., Jaffe, D., Gao, R., Stith, J., Ryerson, T., Aikin, K., Campos, T., Weinheimer, A. and Avery, M. A.: Increasing springtime ozone mixing ratios in the free troposphere over western North America, Nature, 463(7279), 344–348, doi:10.1038/nature08708, 2010.

Cooper, O. R., Gao, R.-S., Tarasick, D., Leblanc, T. and Sweeney, C.: Long-term ozone trends at rural ozone monitoring sites across the United States, 1990-2010, J. Geophys. Res., 117(D22), n/a–n/a, doi:10.1029/2012JD018261, 2012.

Cooper, O. R., Parrish, D. D., Ziemke, J., Balashov, N. V., Cupeiro, M., Galbally, I. E., Gilge, S., Horowitz, L., Jensen, N. R., Lamarque, J.-F., Naik, V., Oltmans, S. J., Schwab, J., Shindell, D. T., Thompson, A. M., Thouret, V., Wang, Y. and Zbinden, R. M.: Global distribution and trends of tropospheric ozone: An observation-based review, Elem. Sci. Anthr., 2, 000029, doi:10.12952/journal.elementa.000029, 2014.

Cui, J., Sprenger, M., Staehelin, J., Siegrist, A., Kunz, M., Henne, S. and Steinbacher, M.: Impact of stratospheric intrusions and intercontinental transport on ozone at Jungfraujoch in 2005: comparison and validation of two Lagrangian approaches, Atmos. Chem. Phys., 9(10), 3371–3383, doi:10.5194/acp-9-3371-2009, 2009.

Danielsen, E. F. and Mohnen, V. A.: Project dustorm report: ozone transport, in situ measurements, and meteorological analyses of tropopause folding, J. Geophys. Res., 82(37), 5867–5877, doi:10.1029/JC082i037p05867, 1977.

Davies, T. D. and Schuepbach, E.: Episodes of high ozone concentrations at the earth's surface resulting from transport down from the upper troposphere/lower stratosphere: a review and case studies, Atmos. Environ., 28(1), 53–68, doi:10.1016/1352-2310(94)90022-1, 1994.

Derwent, R. G., Simmonds, P. G., Manning, A. J. and Spain, T. G.: Trends over a 20-year period from 1987

809 to 2007 in surface ozone at the atmospheric research station, Mace Head, Ireland, Atmos. Environ.,
810 41(39), 9091–9098, doi:10.1016/j.atmosenv.2007.08.008, 2007.

811 Draxler, R., Stunder, B., Rolph, G. and Taylor, A.: Hysplit 4 User's Guide, NOAA Air Resources Laboratory,
812 Silver Spring, 2009.

813 Dufour, G., Eremenko, M., Orphal, J. and Flaud, J.-M.: IASI observations of seasonal and day-to-day
814 variations of tropospheric ozone over three highly populated areas of China: Beijing, Shanghai, and Hong
815 Kong, Atmos. Chem. Phys., 10(8), 3787–3801, doi:10.5194/acp-10-3787-2010, 2010.

816 Engström, A. and Magnusson, L.: Estimating trajectory uncertainties due to flow dependent errors in the
817 atmospheric analysis, Atmos. Chem. Phys., 9, 8857–8867, doi:10.5194/acp-9-8857-2009,2009.

818 Feister, U. and Warmbt, W.: Long-term measurements of surface ozone in the German Democratic
819 Republic, J. Atmos. Chem., 5(1), 1–21, doi:10.1007/BF00192500, 1987.

820 Forster, P., Ramaswamy, V., Artaxo, P., Bernstsen, T., Betts, R., Fahey, D. W., Haywood, J., Lean, J., Lowe,
821 D. W., Myhre, G., Nganga, J., Prinn, R., Raga, G., Schulz, M. and Van Dorland, R.: Changes in atmospheric
822 constituents and in radiative forcing. Chapter 2, Cambridge University Press, Cambridge, United
823 Kingdom and New York, NY, USA., 2007.

824 Gallardo, L., Carrasco, J. and Olivares, G.: An analysis of ozone measurements at Cerro Tololo (30
825 degrees S, 70 degrees W, 2200 m.a.s.l.) in Chile, Tellus B, 52(1), 50–59, doi:10.1034/j.1600-
826 0889.2000.00959.x, 2000.

827 Gao, J., Wang, T., Ding, A. and Liu, C.: Observational study of ozone and carbon monoxide at the summit
828 of mount Tai (1534m a.s.l.) in central-eastern China, Atmos. Environ., 39(26), 4779–4791,
829 doi:10.1016/j.atmosenv.2005.04.030, 2005.

830 Granier, C., Bessagnet, B., Bond, T., D'Angiola, A., Denier van der Gon, H., Frost, G. J., Heil, A., Kaiser, J.
831 W., Kinne, S., Klimont, Z., Kloster, S., Lamarque, J.-F., Liousse, C., Masui, T., Meleux, F., Mieville, A.,
832 Ohara, T., Raut, J.-C., Riahi, K., Schultz, M. G., Smith, S. J., Thompson, A., van Aardenne, J., van der Werf,
833 G. R. and van Vuuren, D. P.: Evolution of anthropogenic and biomass burning emissions of air pollutants
834 at global and regional scales during the 1980–2010 period, Clim. Change, 109(1-2), 163–190,
835 doi:10.1007/s10584-011-0154-1, 2011.

836 Huntzicker, J. J. and Johnson, R. L.: Investigation of an ambient interference in the measurement of
837 ozone by ultraviolet absorption photometry, Environ. Sci. Technol., 13, 1414–1416,
838 doi:10.1021/es60159a005, 1979.

839 Jacob, D. J., Logan, J. A. and Murti, P. P.: Effect of rising Asian emissions on surface ozone in the United
840 States, Geophys. Res. Lett., 26(14), 2175–2178, doi:10.1029/1999GL900450, 1999.

841 Jaffe, D., Price, H., Parrish, D., Goldstein, A., and Harris, J.: Increasing background ozone during spring on
842 the west coast of North America, Geophys. Res. Lett., 30, 1613, doi:10.1029/2003GL017024, 2003.

843 Jaffe, D., Bertschi, I., Jaeglé, L., Novelli, P., Reid, J. S., Tanimoto, H., Vingarzan, R. and Westphal, D. L.:
844 Long-range transport of Siberian biomass burning emissions and impact on surface ozone in western
845 North America, Geophys. Res. Lett., 31(16), L16106, doi:10.1029/2004GL020093, 2004.

846 Ladstätter-Weißenmayer, A., Meyer-Arnek, J., Schlemm, A. and Burrows, J. P.: Influence of stratospheric
847 airmasses on tropospheric vertical O_3 columns based on GOME (Global Ozone Monitoring Experiment)
848 measurements and backtrajectory calculation over the Pacific, Atmos. Chem. Phys., 4(4), 903–909,
849 doi:10.5194/acp-4-903-2004, 2004.

Langford, A. O., Brioude, J., Cooper, O. R., Senff, C. J., Alvarez, R. J., Hardesty, R. M., Johnson, B. J. and Oltmans, S. J.: Stratospheric influence on surface ozone in the Los Angeles area during late spring and early summer of 2010, J. Geophys. Res., 117(D21), n/a–n/a, doi:10.1029/2011JD016766, 2012.

Langford, A. O., Pierce, R. B. and Schultz, P. J.: Stratospheric intrusions, the Santa Ana winds, and wildland fires in Southern California, Geophys. Res. Lett., n/a–n/a, doi:10.1002/2015GL064964, 2015.

Law, K. S., Plantevin, P.-H., Thouret, V., Marenco, A., Asman, W. A. H., Lawrence, M., Crutzen, P. J., Muller, J.-F., Hauglustaine, D. A. and Kanakidou, M.: Comparison between global chemistry transport model results and Measurement of Ozone and Water Vapor by Airbus In-Service Aircraft (MOZAIC) data, J. Geophys. Res., 105(D1), 1503, doi:10.1029/1999JD900474, 2000.

Leblanc, T., McDermid, I. S. and Walsh, T. D.: Ground-based water vapor raman lidar measurements up to the upper troposphere and lower stratosphere for long-term monitoring, Atmos. Meas. Tech., 5(1), 17–36, doi:10.5194/amt-5-17-2012, 2012.

Lee, S. and Akimoto, H.: Lower tropospheric ozone trend observed in 1989–1997 at Okinawa, Japan, Geophys. Res. Lett., 25(10), 1998.

Lefohn, A. S., Wernli, H., Shadwick, D., Limbach, S., Oltmans, S. J. and Shapiro, M.: The importance of stratospheric–tropospheric transport in affecting surface ozone concentrations in the western and northern tier of the United States, Atmos. Environ., 45(28), 4845–4857, doi:10.1016/j.atmosenv.2011.06.014, 2011.

Lefohn, A. S., Wernli, H., Shadwick, D., Oltmans, S. J. and Shapiro, M.: Quantifying the importance of stratospheric-tropospheric transport on surface ozone concentrations at high- and low-elevation monitoring sites in the United States, Atmos. Environ., 62, 646–656, doi:10.1016/j.atmosenv.2012.09.004, 2012.

Lelieveld, J., van Aardenne, J., Fischer, H., de Reus, M., Williams, J. and Winkler, P.: Increasing ozone over the Atlantic Ocean., Science, 304(5676), 1483–7, doi:10.1126/science.1096777, 2004.

Levy, H., Mahlman, J. D., Moxim, W. J. and Liu, S. C.: Tropospheric ozone: The role of transport, J. Geophys. Res., 90(D2), 3753, doi:10.1029/JD090iD02p03753, 1985.

Liang, Q., Jaeglé, L., Jaffe, D. A., Weiss-Penzias, P., Heckman, A. and Snow, J. A.: Long-range transport of Asian pollution to the northeast Pacific: Seasonal variations and transport pathways of carbon monoxide, J. Geophys. Res., 109(D23), n/a–n/a, doi:10.1029/2003JD004402, 2004.

Lin, M., Fiore, A. M., Cooper, O. R., Horowitz, L. W., Langford, A. O., Levy, H., Johnson, B. J., Naik, V., Oltmans, S. J. and Senff, C. J.: Springtime high surface ozone events over the western United States: Quantifying the role of stratospheric intrusions, J. Geophys. Res., 117(D21), n/a–n/a, doi:10.1029/2012JD018151, 2012a.

Lin, M., Fiore, A. M., Horowitz, L. W., Cooper, O. R., Naik, V., Holloway, J., Johnson, B. J., Middlebrook, A. M., Oltmans, S. J., Pollack, I. B., Ryerson, T. B., Warner, J. X., Wiedinmyer, C., Wilson, J. and Wyman, B.: Transport of Asian ozone pollution into surface air over the western United States in spring, J. Geophys. Res., 117(4), 1–20, doi:10.1029/2011JD016961, 2012b.

Lin, M., Horowitz, L.W., Oltmans, S. J., Fiore, A. M. and Fan, S.: Tropospheric ozone trends at Mauna Loa Observatory tied to decadal climate variability,Nature Geoscience, 7, 136-143, doi:10.1038/NGEO2066, 2014.

Lin, M., Fiore, A. M., Horowitz, L. W., Langford, A. O., Oltmans, S. J., Tarasick, D. and Rieder, H. E.:

Climate variability modulates western US ozone air quality in spring via deep stratospheric intrusions., Nat. Commun., 6, 7105, doi:10.1038/ncomms8105, 2015a.

Lin, M., Horowitz, L.W., Cooper, O.R., Tarasick, D., Conley, S., Iraci, L.T., Johnson, B., Leblanc, T., Petropavlovskikh, I., and Yates, E.L.: Revisiting the evidence of increasing springtime ozone mixing ratios in the free troposphere over western North America, Geophysical Research Letter, 42, doi:10.1002/2015GL065311, 2015b.

Logan, J. A.: Trends in the vertical distribution of ozone: An analysis of ozonesonde data, J. Geophys. Res., 99(D12), 25553, doi:10.1029/94JD02333, 1994.

Logan J.A., J. Staehelin, I. A. Megretskaia, J.-P. Cammas, V. Thouret, H. Claude, H. De Backer, M. Steinbacher, H. E. Scheel, R. Stübi, M. Fröhlich, and R. Derwent, Changes in ozone over Europe since 1990: analysis of ozone measurements from sondes, regular aircraft (MOZAIC) and alpine surface sites. J. Geophys. Res., D09301, doi:10.1029/2011JD016952, 2012.

Logan, J. A., Megretskaia, I. A., Miller, A. J., Tiao, G. C., Choi, D., Zhang, L., Stolarski, R. S., Labow, G. J., Hollandsworth, S. M., Bodeker, G. E., Claude, H., De Muer, D., Kerr, J. B., Tarasick, D. W., Oltmans, S. J., Johnson, B., Schmidlin, F., Staehelin, J., Viatte, P. and Uchino, O.: Trends in the vertical distribution of ozone: A comparison of two analyses of ozonesonde data, J. Geophys. Res., 104(D21), 26373, doi:10.1029/1999JD900300, 1999.

McDermid, I. S.: Differential absorption lidar systems for tropospheric and stratospheric ozone measurements, Opt. Eng., 30(1), 22, doi:10.1117/12.55768, 1991.

McDermid, S., Beyerle, G., Haner, D. a and Leblanc, T.: Redesign and improved performance of the tropospheric ozone lidar at the Jet Propulsion Laboratory Table Mountain Facility., Appl. Opt., 41(36), 7550–7555, 2002.

Mickley, L. J., Jacob, D. J. and Rind, D.: Uncertainty in preindustrial abundance of tropospheric ozone: Implications for radiative forcing calculations, J. Geophys. Res., 106(D4), 3389, doi:10.1029/2000JD900594, 2001.

Monks, P.: Gas-phase radical chemistry in the troposphere, Chem. Soc. Rev., 2005.

Naja, M. and Akimoto, H.: Contribution of regional pollution and long-range transport to the Asia-Pacific region: Analysis of long-term ozonesonde data over Japan, J. Geophys. Res., 109(D21), D21306, doi:10.1029/2004JD004687, 2004.

Naja, M., Lal, S. and Chand, D.: Diurnal and seasonal variabilities in surface ozone at a high altitude site Mt Abu (24.6??N, 72.7??E, 1680 m asl) in India, Atmos. Environ., 37(30), 4205–4215, doi:10.1016/S1352-2310(03)00565-X, 2003.

Neu, J. L., Flury, T., Manney, G. L., Santee, M. L., Livesey, N. J. and Worden, J.: Tropospheric ozone variations governed by changes in stratospheric circulation, Nat. Geosci., 7(5), 340–344, doi:10.1038/ngeo2138, 2014.

Neuman, J. A., Trainer, M., Aikin, K. C., Angevine, W. M., Brioude, J., Brown, S. S., de Gouw, J. A., Dube, W. P., Flynn, J. H., Graus, M., Holloway, J. S., Lefer, B. L., Nedelec, P., Nowak, J. B., Parrish, D. D., Pollack, I. B., Roberts, J. M., Ryerson, T. B., Smit, H., Thouret, V., and Wagner, N. L.: Observations of ozone transport from the free troposphere to the Los Angeles basin, J. Geophys. Res., 117, D00V09, doi: 10.1029/2011JD016919, 2012.

Newchurch, M. J., M. A. Ayoub, S. Oltmans, B. Johnson, and F. J. Schmidlin, Vertical distribution of ozone

at four sites in the United States, J. Geophys. Res., 108(D1), 4031, doi:10.1029/2002JD002059, 2003.

Oltmans, S. J. and Komhyr, W. D.: Surface ozone distributions and variations from 1973–1984: Measurements at the NOAA Geophysical Monitoring for Climatic Change Baseline Observatories, J. Geophys. Res., 91(D4), 5229, doi:10.1029/JD091iD04p05229, 1986.

Oltmans, S. J., Lefohn, A. S., Scheel, H. E., Harris, J. M., Levy, H., Galbally, I. E., Brunke, E.-G., Meyer, C. P., Lathrop, J. A., Johnson, B. J., Shadwick, D. S., Cuevas, E., Schmidlin, F. J., Tarasick, D. W., Claude, H., Kerr, J. B., Uchino, O. and Mohnen, V.: Trends of ozone in the troposphere, Geophys. Res. Lett., 25(2), 139–142, doi:10.1029/97GL03505, 1998.

Oltmans, S. J., Lefohn, A. S., Harris, J. M., Galbally, I., Scheel, H. E., Bodeker, G., Brunke, E., Claude, H., Tarasick, D., Johnson, B. J., Simmonds, P., Shadwick, D., Anlauf, K., Hayden, K., Schmidlin, F., Fujimoto, T., Akagi, K., Meyer, C., Nichol, S., Davies, J., Redondas, A. and Cuevas, E.: Long-term changes in tropospheric ozone, Atmos. Environ., 40(17), 3156–3173, doi:10.1016/j.atmosenv.2006.01.029, 2006.

Oltmans, S. J., Lefohn, a. S., Shadwick, D., Harris, J. M., Scheel, H. E., Galbally, I., Tarasick, D. W., Johnson, B. J., Brunke, E. G., Claude, H., Zeng, G., Nichol, S., Schmidlin, F., Davies, J., Cuevas, E., Redondas, a., Naoe, H., Nakano, T. and Kawasato, T.: Recent tropospheric ozone changes - A pattern dominated by slow or no growth, Atmos. Environ., 67, 331–351, doi:10.1016/j.atmosenv.2012.10.057, 2013.

Parrish, D., Dunlea, E. J., Atlas, E. L., Schauffler, S., Donnelly, S., Stroud, V., Goldstein, A. H., Millet, D. B., McKay, M., Jaffe, D. A., Price, H. U., Hess, P. G., Flocke, F., and Roberts, J. M.: Changes in the photochemical environment of the temperate North Pacific troposphere in response to increased Asian emissions, J. Geophys. Res., 109, D23S18, doi: 10.1029/2004JD004978, 2004.

Parrish, D. D., Millet, D. B., Goldstein, A. H. and Division, C. S.: Increasing ozone in marine boundary layer inflow at the west coasts of North America and Europe, Atmos. Chem. Phys., 1303–1323, doi:10.5194/acp-9-1303-2009, 2009.

Parrish, D. D., Law, K. S., Staehelin, J., Derwent, R., Cooper, O. R., Tanimoto, H., Volz-Thomas, A., Gilge, S., Scheel, H.-E., Steinbacher, M. and Chan, E.: Long-term changes in lower tropospheric baseline ozone concentrations at northern mid-latitudes, Atmos. Chem. Phys., 12(23), 11485–11504, doi:10.5194/acp-12-11485-2012, 2012.

Petetin, H., Thouret, V., Fontaine, A., Sauvage, B., Athier, G., Blot, R., Boulanger, D., Cousin, J.-M. and Nedelec, P.: Characterizing tropospheric ozone and CO around Frankfurt between 1994–2012 based on MOZAIC-IAGOS aircraft measurements, Atmos. Chem. Phys. Discuss., 15(17), 23841–23891, doi:10.5194/acpd-15-23841-2015, 2015.

Pochanart, P., Hirokawa, J. and Kajii, Y.: Influence of regional-scale anthropogenic activity in northeast Asia on seasonal variations of surface ozone and carbon monoxide observed at Oki, Japan, J. Geophys. Res., *104*(D3), 3621-3631, 1999.

Michael H. Proffitt and Andrew O. Langford, Ground-based differential absorption lidar system for day or night measurements of ozone throughout the free troposphere, Appl. Opt. 36, 2568-2585, 1997.

Randel, W. J., D. J. Seidel, and L. L. Pan, Observational characteristics of double tropopauses, J. Geophys. Res., 112, D07309, doi:10.1029/2006JD007904, 2007.

Reidmiller, D. R., Fiore, A. M., Jaffe, D. A., Bergmann, D., Cuvelier, C., Dentener, F. J., Duncan, B. N., Folberth, G., Gauss, M., Gong, S., Hess, P., Jonson, J. E., Keating, T., Lupu, A., Marmer, E., Park, R., Schultz, M. G., Shindell, D. T., Szopa, S., Vivanco, M. G., Wild, O. and Zuber, A.: The influence of foreign

vs. North American emissions on surface ozone in the US, Atmos. Chem. Phys., 9(14), 5027–5042, doi:10.5194/acp-9-5027-2009, 2009.

Rienecker, M.M., M.J. Suarez, R. Gelaro, R. Todling, J. Bacmeister, E. Liu, M.G. Bosilovich, S.D. Schubert, L. Takacs, G.-K. Kim, S. Bloom, J. Chen, D. Collins, A. Conaty, A. da Silva, W. Gu, J. Joiner, R.D. Koster, R. Lucchesi, A. MOlod, T. Owens. S. Pawson, P. Pegion, C. R. Redder, R. Reichle, F. R. Robertson A. G. Ruddick, M. Sienkiewicz and J. Woolen: MERRA: NASA's Modern-Era Retrospective Analysis for Research and Applications. J. Climate, 24, 3624-3648, doi:10.1175/JCLI-D-11-00015.1, 2011.

Roelofs, G.-J. and Lelieveld, J.: Model study of the influence of cross-tropopause O3 transports on tropospheric O3 levels, Tellus B, 49(1), 38–55, doi:10.1034/j.1600-0889.49.issue1.3.x, 1997.

Simmonds, P. G., Derwent, R. G., Manning, A. L. and Spain, G.: Significant growth in surface ozone at Mace Head, Ireland, 1987–2003, Atmos. Environ., 38(28), 4769–4778, doi:10.1016/j.atmosenv.2004.04.036, 2004.

Sinha, V., Kumar, V., and Sarkar, C.: Chemical composition of pre-monsoon air in the Indo-Gangetic Plain measured using a new air quality facility and PTR-MS: high surface ozone and strong influence of biomass burning, Atmos. Chem. Phys., 14, 5921-5941, doi:10.5194/acp-14-5921-2014, 2014.

Smit, H. G. J., Straeter, W., Johnson, B. J., Oltmans, S. J., Davies, J., Tarasick, D. W., Hoegger, B., Stubi, R., Schmidlin, F. J., Northam, T., Thompson, A. M., Witte, J. C., Boyd, I. and Posny, F.: Assessment of the performance of ECC-ozonesondes under quasi-flight conditions in the environmental simulation chamber: Insights from the Juelich Ozone Sonde Intercomparison Experiment (JOSIE), J. Geophys. Res., 112(D19), D19306, doi:10.1029/2006JD007308, 2007.

Sprenger, M.: A northern hemispheric climatology of cross-tropopause exchange for the ERA15 time period (1979–1993), J. Geophys. Res., 108(D12), 8521, doi:10.1029/2002JD002636, 2003.

Staehelin, J., Thudium, J., Buehler, R., Volz-Thomas, A. and Graber, W.: Trends in surface ozone concentrations at Arosa (Switzerland), Atmos. Environ., 28(1), 75–87, doi:10.1016/1352-2310(94)90024-8, 1994.

Stevenson, D. S., Dentener, F. J., Schultz, M. G., Ellingsen, K., van Noije, T. P. C., Wild, O., Zeng, G., Amann, M., Atherton, C. S., Bell, N., Bergmann, D. J., Bey, I., Butler, T., Cofala, J., Collins, W. J., Derwent, R. G., Doherty, R. M., Drevet, J., Eskes, H. J., Fiore, A. M., Gauss, M., Hauglustaine, D. A., Horowitz, L. W., Isaksen, I. S. A., Krol, M. C., Lamarque, J.-F., Lawrence, M. G., Montanaro, V., Müller, J.-F., Pitari, G., Prather, M. J., Pyle, J. A., Rast, S., Rodriguez, J. M., Sanderson, M. G., Savage, N. H., Shindell, D. T., Strahan, S. E., Sudo, K. and Szopa, S.: Multimodel ensemble simulations of present-day and near-future tropospheric ozone, J. Geophys. Res., 111(D8), D08301, doi:10.1029/2005JD006338, 2006.

Stohl, A.: On the pathways and timescales of intercontinental air pollution transport, J. Geophys. Res., 107(D23), 4684, doi:10.1029/2001JD001396, 2002.

Stohl, A.: Stratosphere-troposphere exchange: A review, and what we have learned from STACCATO, J. Geophys. Res., 108(D12), 8516, doi:10.1029/2002JD002490, 2003.

Strode, S. A., Rodriguez, J. M., Logan, J. A., Cooper, O. R., Witte, J. C., Lamsal, L. N., Damon, M., Van Aartsen, B., Steenrod, S. D. and Strahan, S. E.: Trends and variability in surface ozone over the United States, J. Geophys. Res., 120(17), n/a–n/a, doi:10.1002/2014JD022784, 2015.

Tanimoto, H., Ohara, T. and Uno, I.: Asian anthropogenic emissions and decadal trends in springtime tropospheric ozone over Japan: 1998–2007, Geophys. Res. Lett., 36(23), L23802, doi:10.1029/2009GL041382, 2009.

The Royal Society, T.: Ground-level ozone in the 21st century: future trends, impacts and policy implications., 2008.

Thompson, A. M., Stone, J. B., Witte, J. C., Miller, S. K., Oltmans, S. J., Kucsera, T. L., Ross, K. L., Pickering, K. E., Merrill, J. T., Forbes, G., Tarasick, D. W., Joseph, E., Schmidlin, F. J., McMillan, W. W., Warner, J., Hintsa, E. J. and Johnson, J. E.: Intercontinental Chemical Transport Experiment Ozonesonde Network Study (IONS) 2004: 2. Tropospheric ozone budgets and variability over northeastern North America, J. Geophys. Res., 112(D12), D12S13, doi:10.1029/2006JD007670, 2007.

Tie, X., Geng, F., Peng, L., Gao, W. and Zhao, C.: Measurement and modeling of O3 variability in Shanghai, China: Application of the WRF-Chem model, Atmos. Environ., 43(28), 4289–4302, doi:10.1016/j.atmosenv.2009.06.008, 2009.

Trickl, T., Feldmann, H., Kanter, H.-J., Scheel, H.-E., Sprenger, M., Stohl, A. and Wernli, H.: Forecasted deep stratospheric intrusions over Central Europe: case studies and climatologies, Atmos. Chem. Phys., 10(2), 499–524, doi:10.5194/acp-10-499-2010, 2010.

Trickl, T., Bärtsch-Ritter, N., Eisele, H., Furger, M., Mücke, R., Sprenger, M. and Stohl, A.: High-ozone layers in the middle and upper troposphere above Central Europe: potential import from the stratosphere along the subtropical jet stream, Atmos. Chem. Phys., 11(17), 9343–9366, doi:10.5194/acp-11-9343-2011, 2011.

Tsutsumi, Y. and Matsueda, H.: Relationship of ozone and CO at the summit of Mt. Fuji (35.35°N, 138.73°E, 3776m above sea level) in summer 1997, Atmos. Environ., 34(4), 553–561, doi:10.1016/S1352-2310(99)00238-1, 2000.

Vaughan, G., Price, J. D. and Howells, A.: Transport into the troposphere in a tropopause fold, Q. J. R. Meteorol. Soc., 120(518), 1085–1103, doi:10.1002/qj.49712051814, 1994.

Volz, A. and Kley, D.: Evaluation of the Montsouris series of ozone measurements made in the nineteenth century, Nature, 332(6161), 240–242, doi:10.1038/332240a0, 1988.

Wang, T., Ding, A., Gao, J. and Wu, W. S.: Strong ozone production in urban plumes from Beijing, China, Geophys. Res. Lett., 33(21), L21806, doi:10.1029/2006GL027689, 2006.

WMO (World Meteorological Organization), A three-dimensional science: Second session of the commission for aerology, WMO Bull., IV, 1957.

WMO (World Meteorological Organization), *Scientific Assessment of Ozone Depletion: 2014*, World Meteorological Organization, Global Ozone Research and Monitoring Project-Report No. 55, 416 pp., Geneva, Switzerland, 2014

World Health Organization: Health aspects of air pollution with particulate matter, ozone and nitrogen dioxide: report on a WHO working group, Bonn, Germany 13-15 January 2003., 2003.

Yates, E. L., Iraci, L. T., Roby, M. C., Pierce, R. B., Johnson, M. S., Reddy, P. J., Tadić, J. M., Loewenstein, M. and Gore, W.: Airborne observations and modeling of springtime stratosphere-to- troposphere transport over California, Atmos. Chem. Phys., 13(24), 12481–12494, doi:10.5194/acp-13-12481-2013, 2013.

Young, P. J., Archibald, A. T., Bowman, K. W., Lamarque, J.-F., Naik, V., Stevenson, D. S., Tilmes, S., Voulgarakis, A., Wild, O., Bergmann, D., Cameron-Smith, P., Cionni, I., Collins, W. J., Dalsøren, S. B., Doherty, R. M., Eyring, V., Faluvegi, G., Horowitz, L. W., Josse, B., Lee, Y. H., MacKenzie, I. A., Nagashima, T., Plummer, D. A., Righi, M., Rumbold, S. T., Skeie, R. B., Shindell, D. T., Strode, S. A., Sudo, K., Szopa, S.

and Zeng, G.: Pre-industrial to end 21st century projections of tropospheric ozone from the Atmospheric Chemistry and Climate Model Intercomparison Project (ACCMIP), Atmos. Chem. Phys., 13(4), 2063–2090, doi:10.5194/acp-13-2063-2013, 2013.

Zbinden, R. M., Cammas, J.-P., Thouret, V., Nédélec, P., Karcher, F. and Simon, P.: Mid-latitude tropospheric ozone columns from the MOZAIC program: climatology and interannual variability, Atmos. Chem. Phys., 6(4), 1053–1073, doi:10.5194/acp-6-1053-2006, 2006.

Zhang, L., Jacob, D. J., Boersma, K. F., Jaffe, D. A., Olson, J. R., Bowman, K. W., Worden, J. R., Thompson, A. M., Avery, M. A., Cohen, R. C., Dibb, J. E., Flock, F. M., Fuelberg, H. E., Huey, L. G., McMillan, W. W., Singh, H. B., and Weinheimer, A. J.: Transpacific transport of ozone pollution and the effect of recent Asian emission increases on air quality in North America: an integrated analysis using satellite, aircraft, ozonesonde, and surface observations, Atmos. Chem. Phys., 8, 6117-6136, doi:10.5194/acp-8-6117-2008, 2008.

Zhang, L., Jacob, D. J., Liu, X., Logan, J. A., Chance, K., Eldering, A. and Bojkov, B. R.: Intercomparison methods for satellite measurements of atmospheric composition: application to tropospheric ozone from TES and OMI, Atmos. Chem. Phys., 10(10), 4725–4739, doi:10.5194/acp-10-4725-2010, 2010.

Zbinden R.M., V. Thouret, P. Ricaud, F. Carminati, J.-P. Cammas, and P. Nédélec, Climatology of pure tropospheric profiles and column contents of ozone and carbon monoxide using MOZAIC in the mid-northern latitudes (24_ N to 50_ N) from 1994 to 2009„ Atmos. Chem. Phys., 13, 12363-12388, doi:10.5194/acp-13-12363-2013, 2013.

Table 1. Number of measurements, by month and years, performed at TMF with the tropospheric ozone DIAL system. N/A indicates data not available at the time of the study

	Jan	Feb	Mar	Apr	May	Jun	Jul	Aug	Sep	Oct	Nov	Dec	Total
2000	4	2	6	4	11	12	7	10	8	1	0	0	65
2001	1	11	17	2	9	13	12	15	15	17	8	10	130
2002	6	10	6	4	0	10	11	1	6	16	12	11	93
2003	11	9	15	12	10	13	5	7	9	14	7	5	117
2004	9	8	15	14	12	6	12	13	11	10	9	11	130
2005	4	6	13	8	12	16	9	2	7	2	11	9	99
2006	11	9	6	8	14	5	2	12	12	20	6	1	106
2007	0	0	4	9	11	7	8	10	8	26	10	8	101
2008	7	11	8	13	9	4	11	10	6	11	4	6	100
2009	14	11	7	5	7	8	4	10	4	17	1	3	91
2010	0	0	3	8	0	7	4	1	4	5	9	3	44
2011	2	6	4	7	7	11	10	12	7	8	8	8	90
2012	0	9	9	1	10	13	3	2	5	8	4	5	69
2013	6	3	5	10	8	7	5	7	0	0	0	0	51
2014	9	2	5	10	13	16	15	11	15	15	14	6	131
2015	9	15	12	18	3	14	12	N/A	N/A	N/A	N/A	N/A	83
Total	93	112	135	133	136	162	130	123	117	170	103	86	1500

Table 2. Ozone mixing ratio trends for the median, 5th and 95th percentiles over the period 2000-2015 as shown in Figure 6 (see text for details) in ppbv·year^{-1} (%·year^{-1}). Statistically significant trends at 95% and 90% confidence level are marked in bold font and underlined respectively.

Ozone mixing ratio trends in ppbv/year (%/year)

	Year			Spring			Summer			Fall			Winter		
	Med.	**5th P.**	**95th P.**	**Med.**	**5th P.**	**95th P.**	**Med.**	**5th P.**	**95th P.**	**Med.**	**5th P.**	**95th P.**	**Med.**	**5th P.**	**95th P.**
17-19 km	-0.49 (-0.05)	0.25 (0.05)	-5.37 (-0.37)	-1.01 (-0.1)	3.47 (0.68)	-5.89 (-0.41)	-2.93 (-0.44)	-3.25 (-0.63)	-0.13 (-0.01)	-8.79 (-1.39)	-5.80 (-1.26)	-6.58 (-0.68)	-0.12 (-0.01)	1.37 (0.27)	-21.86 (-1.51)
12-16 km	1.56 (1.01)	-0.01 (-0.01)	2.52 (0.51)	1.10 (0.50)	0.58 (0.19)	0.29 (0.05)	0.08 (0.06)	0.20 (0.30)	0.19 (0.06)	-0.83 (-0.71)	-1.12 (-1.83)	-1.49 (-0.63)	2.54 (1.31)	0.51 (0.65)	0.95 (0.18)
7-10 km	0.31 (0.57)	0.01 (0.03)	0.55 (0.54)	**0.71 (1.10)**	0.20 (0.49)	4.31 (6.69)	**0.58 (0.98)**	0.27 (0.90)	1.01 (0.95)	-0.03 (-0.06)	-0.49 (1.62)	0.18 (0.22)	**-0.43 (-0.87)**	-0.30 (-0.91)	-1.19 (-1.41)
4-7 km	-0.14 (-0.26)	-0.33 (-0.85)	0.19 (0.17)	0.12 (0.20)	-0.29 (-0.67)	0.96 (1.17)	-0.14 (-0.24)	-0.03 (0.09)	-0.01 (-0.01)	-0.23 (0.45)	-0.82 (-2.33)	0.26 (0.06)	**-0.36 (-0.72)**	**-0.59 (-1.53)**	0.05 (0.08)

Table 3. Standard errors in ppbv·year^{-1} and p-Values associated to ozone mixing ratio trends for the median, 5th and 95th percentiles included in Table 2 and shown in Figure 6. Data corresponding to statistically significant trends at 95% and 90% confidence level are marked in bold font and underlined respectively.

Ozone mixing ratio trend standard errors in ppbv/year (%/year)

	Year			Spring			Summer			Fall			Winter		
	Med.	**5th P.**	**95th P.**	**Med.**	**5th P.**	**95th P.**	**Med.**	**5th P.**	**95th P.**	**Med.**	**5th P.**	**95th P.**	**Med.**	**5th P.**	**95th P.**
17-19 km	3.58	3.12	6.22	6.79	4.76	8.71	2.57	3.88	5.32	4.47	2.92	11.77	7.06	5.90	0.82
	(0.09)	(0.62)	(0.43)	(0.67)	(0.93)	(0.61)	(0.39)	(0.75)	(4.09)	(0.71)	(0.63)	(1.22)	(0.59)	(1.16)	(0.06)
12-16 km	1.21	0.39	4.66	1.83	0.89	5.95	0.83	0.51	3.76	1.10	0.85	3.84	2.54	1.16	10.05
	(0.78)	(0.39)	(0.94)	(0.83)	(0.29)	(1.03)	(0.62)	(0.77)	(1.18)	(0.94)	(1.39)	(1.62)	(1.31)	(1.48)	(1.90)
7-10 km	0.15	0.19	0.30	**0.25**	0.38	3.32	**0.28**	0.20	1.20	0.25	0.35	0.97	**0.18**	0.27	1.00
	(0.28)	(0.57)	(0.29)	**(0.39)**	(0.93)	(5.15)	**(0.47)**	(0.07)	(1.13)	(0.50)	(1.16)	(1.19)	**(0.34)**	(0.82)	(1.60)
4-7 km	0.14	0.24	0.25	0.31	0.36	0.56	0.21	0.35	0.38	0.31	0.38	0.53	**0.16**	**0.18**	0.28
	(0.26)	(0.62)	(0.22)	(0.52)	(0.83)	(0.68)	(0.36)	(1.05)	(0.56)	(0.61)	(1.08)	(0.12)	**(0.32)**	**(0.47)**	(0.45)

p-Values

	Year			Spring			Summer			Fall			Winter		
	Med.	**5th P.**	**95th P.**	**Med.**	**5th P.**	**95th P.**	**Med.**	**5th P.**	**95th P.**	**Med.**	**5th P.**	**95th P.**	**Med.**	**5th P.**	**95th**
17-19 km	0.89	0.94	0.40	0.88	0.48	0.51	0.27	0.41	0.98	0.07	0.07	0.60	0.99	0.82	0.17
12-16 km	0.22	0.98	0.60	0.55	0.52	0.96	0.92	0.71	0.96	0.47	0.21	0.70	0.29	0.67	0.92
7-10 km	0.06	0.94	0.09	**0.01**	0.60	0.22	**0.05**	0.19	0.41	0.91	0.18	0.86	**0.03**	0.28	0.25
4-7 km	0.33	0.19	0.44	0.70	0.44	0.11	0.52	0.92	0.98	0.47	0.05	0.63	**0.04**	**4.10^{-3}**	0.85

Table 4. Number of air parcels ending at TMF during lidar measurements over the period 2000-2015, classified as “Stratosphere”, “Central America, “ABL” (Asian Boundary Layer),”AFT” (Asian Free Troposphere), and “Pacific Ocean” (see text for details)

	Strat	**Cent Am**	**ABL**	**AFT**	**Pac**	**RT**
14 km	1161 (80%)	39 (3%)	0 (0%)	102 (7%)	100 (7%)	55 (4%)
13 km	905 (62%)	57 (4%)	5 (0%)	266 (18%)	139 (10%)	85 (6%)
12 km	658 (45%)	78 (5%)	28 (2%)	425 (29%)	168 (12%)	100 (7%)
11 km	426 (29%)	76 (5%)	49 (3%)	523 (36%)	243 (17%)	140 (10%)
10 km	258 (18%)	86 (6%)	82 (6%)	584 (40%)	304 (21%)	143 (10%)
9 km	167 (11%)	85 (6%)	101 (7%)	613 (42%)	296 (20%)	195 (13%)
8 km	123 (8%)	97 (7%)	124 (9%)	572 (39%)	321 (22%)	220 (15%)
7 km	97 (7%)	107 (7%)	122 (8%)	540 (37%)	317 (22%)	274 (19%)
6 km	69 (5%)	137 (9%)	136 (9%)	499 (34%)	330 (23%)	286 (20%)
5 km	72 (5%)	179 (12%)	107 (7%)	472 (32%)	266 (18%)	361 (25%)

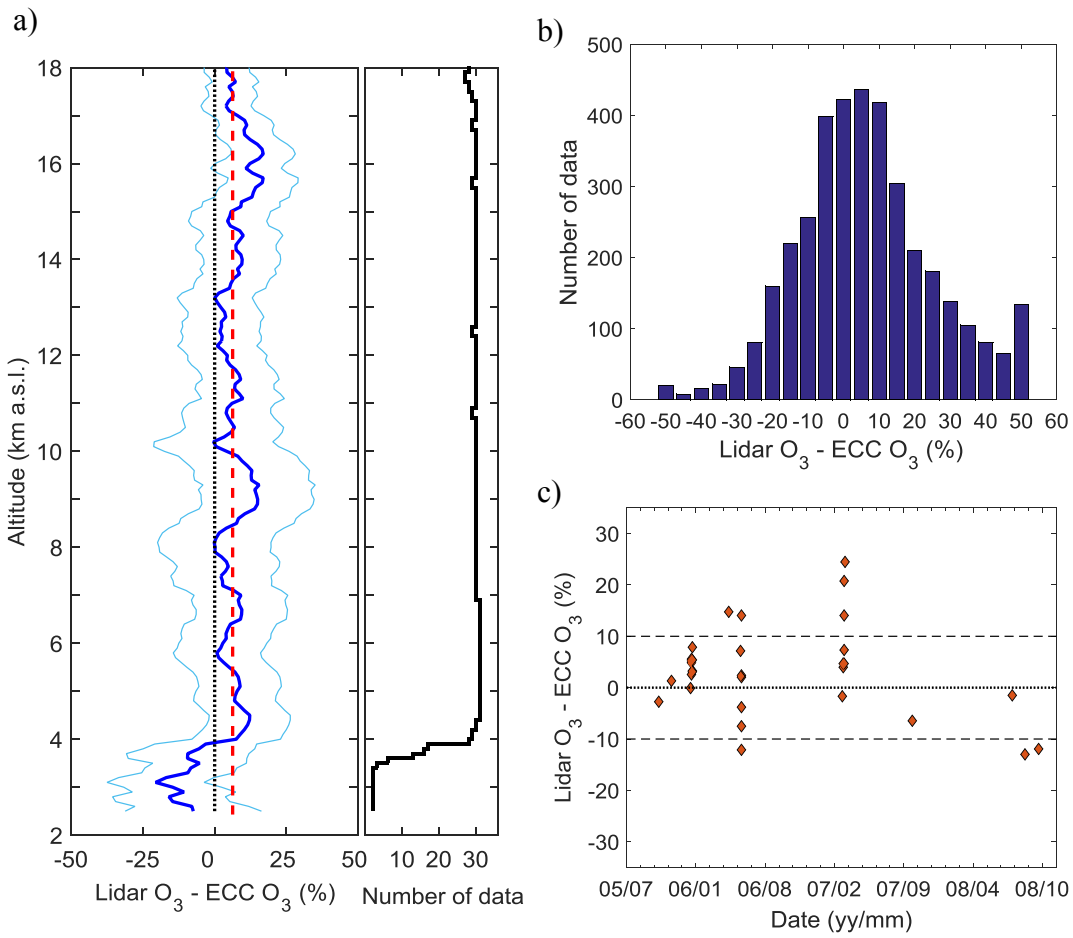

Figure 1. a) Profile of the mean relative difference between the lidar and the ECC ozone number density for the 32 simultaneous measurements (dark blue). Lidar uncertainty (light blue) and mean relative difference obtained between 4 and 16 km (red dotted line) are superimposed. The black solid curve shows the number of data points at each altitude. b) Histogram of the difference between the lidar and the ECC ozone number density. c) Column-averaged (below 8 km) difference between the lidar and the ECC sonde for each coincidence

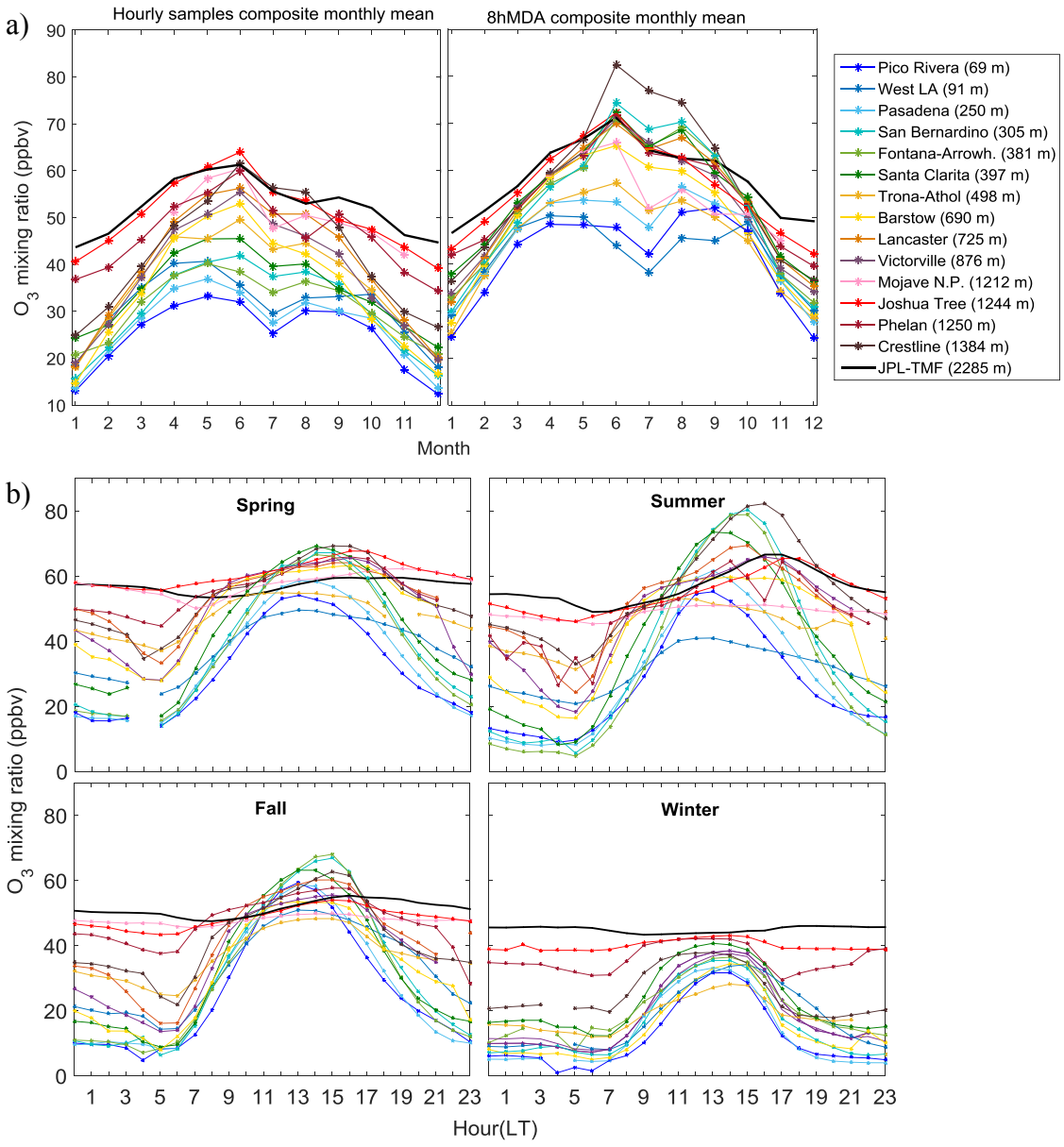

Figure 2. a) Composite monthly mean surface ozone at TMF and nearby ARB stations obtained from hourly samples (left) and 8hMDA values (right) for the period 2013-2015. b) Composite mean ozone daily cycle at TMF and nearby ARB stations for the four seasons for the period 2013-2015

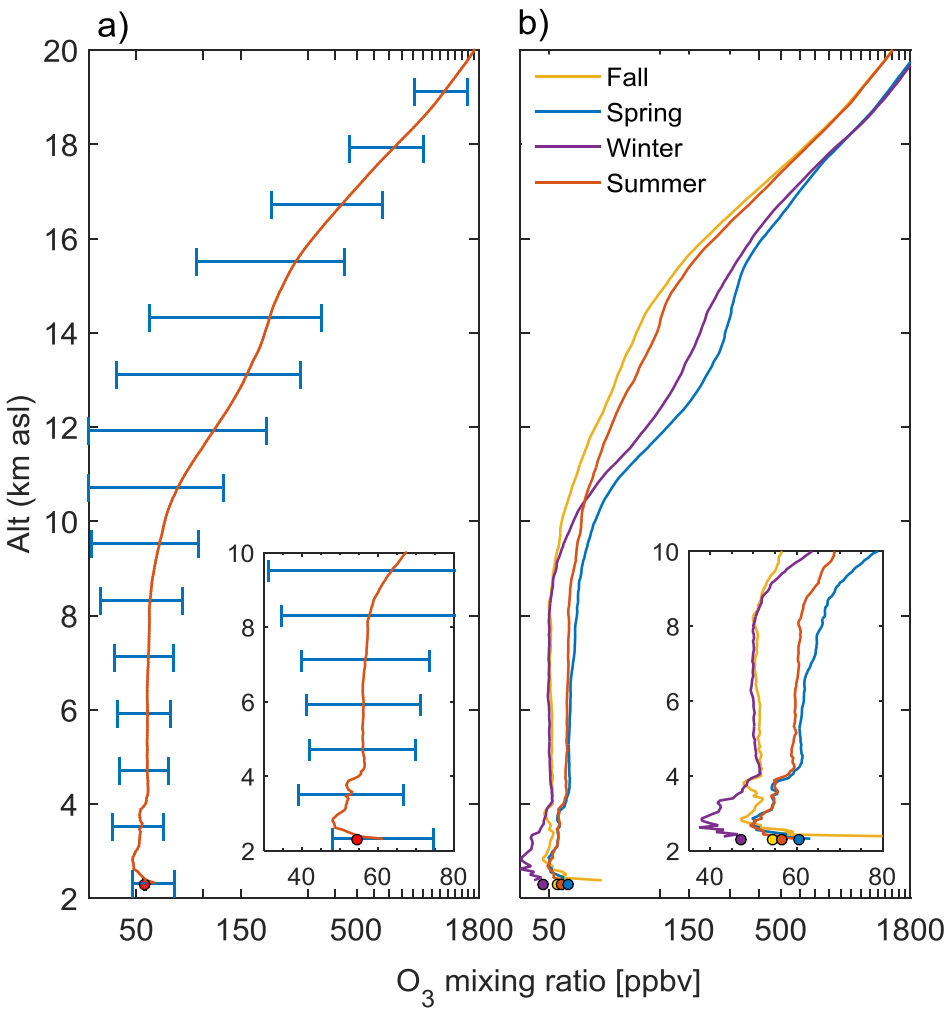

Figure 3. a) Ozone mixing ratio climatological average (2000-2015) computed from the TMF lidar measurements (red curve). The cyan horizontal bars indicate the standard deviation at intervals of 1-km. The red dot at the bottom indicates the mean surface ozone mixing ratio (2013-2015) measured simultaneously with lidar. A zoomed version of the plot focused on the tropospheric part of the profiles (2-10 km) is inserted within the figure. b) Seasonally-averaged ozone mixing ratio profiles for spring (MAM), summer (JJA), fall (SON) and winter (DJF). The dots at the bottom indicate the corresponding surface ozone seasonal averages. A zoomed version of the plot focused on the tropospheric part of the profiles (2-10 km) is inserted within the figure.

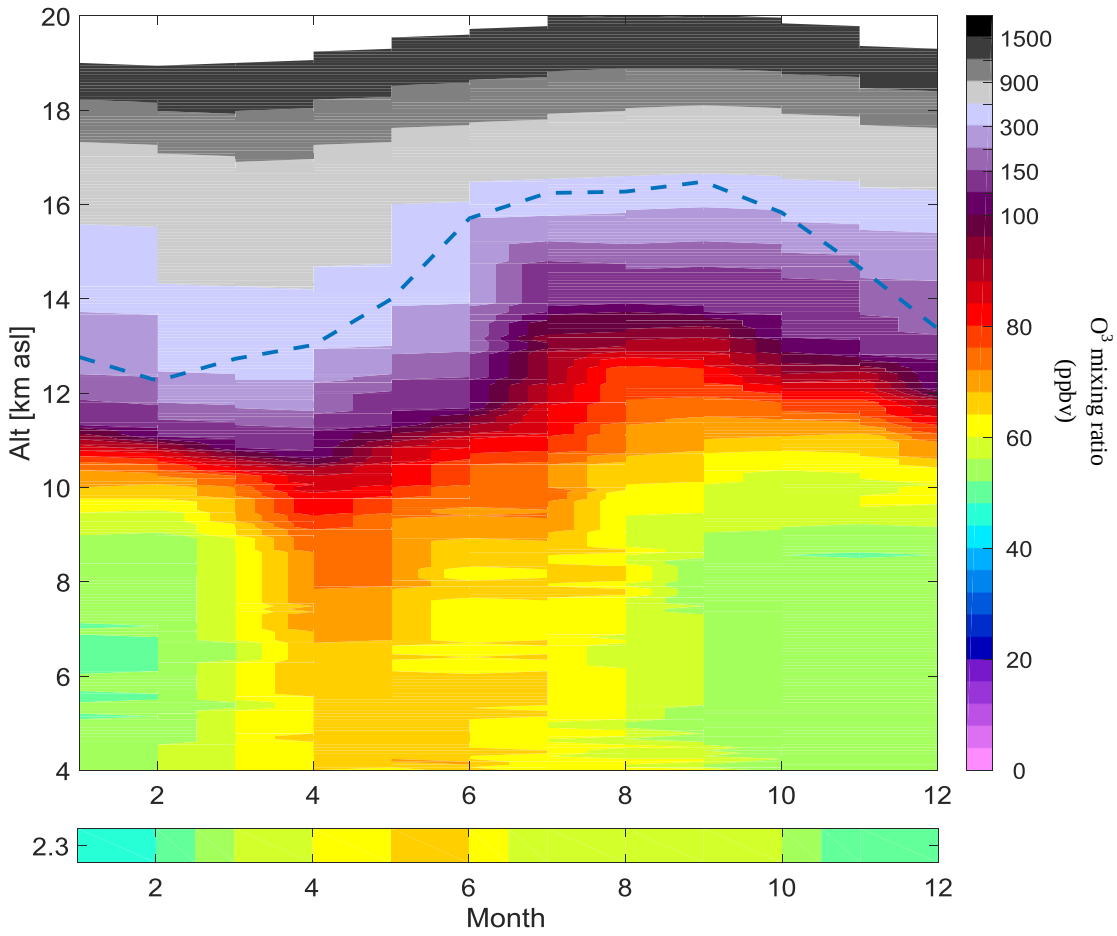

Figure 4. Composite monthly mean ozone mixing ratio (2000-2015) computed from the TMF lidar measurements. The dashed line indicates the climatological tropopause above the site (WMO definition). Bottom strip: Composite monthly mean ozone mixing ratio (2000-2015) from the surface measurements

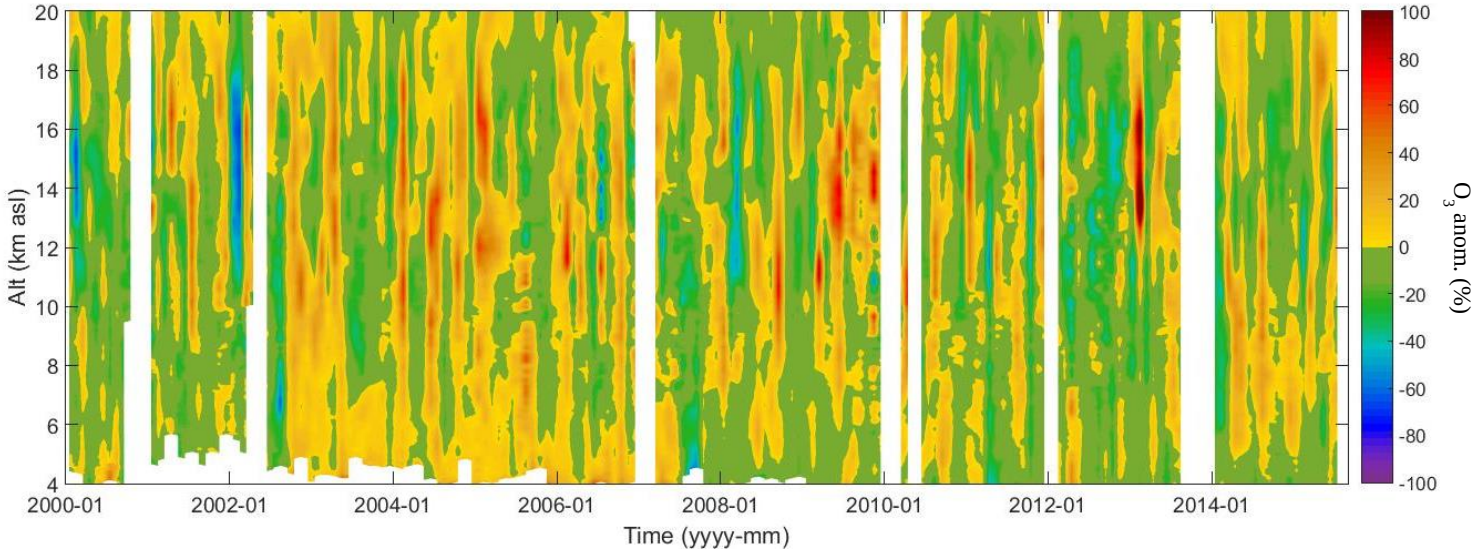

Figure 5. Deseasonalized ozone mixing ratio above TMF. Anomalies (in %) were computed with respect to the climatological (2000-2015) monthly means

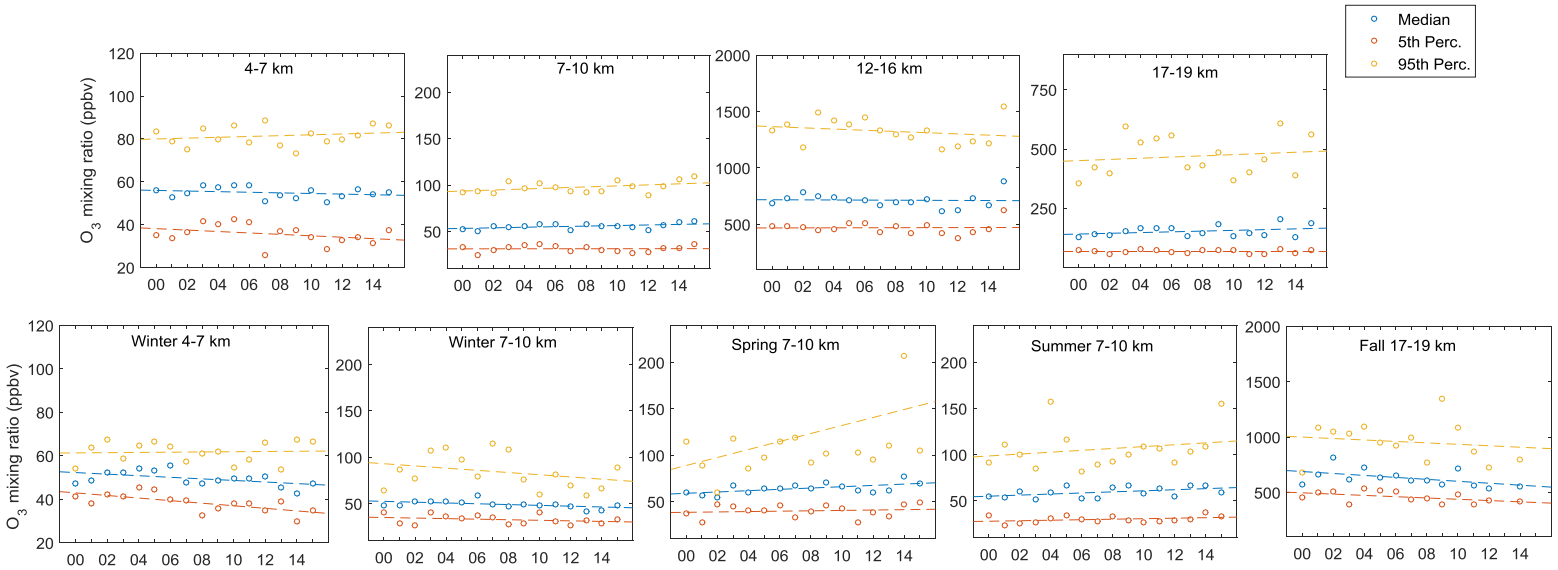

Figure 6. Time series of the median (blue), 5th (orange) and 95th (yellow) percentile ozone values at different altitude layers for the full year (top) and for selected seasons and altitude layers (bottom) obtained from the TMF lidar measurements. Dashed lines represent the linear fit for each time series

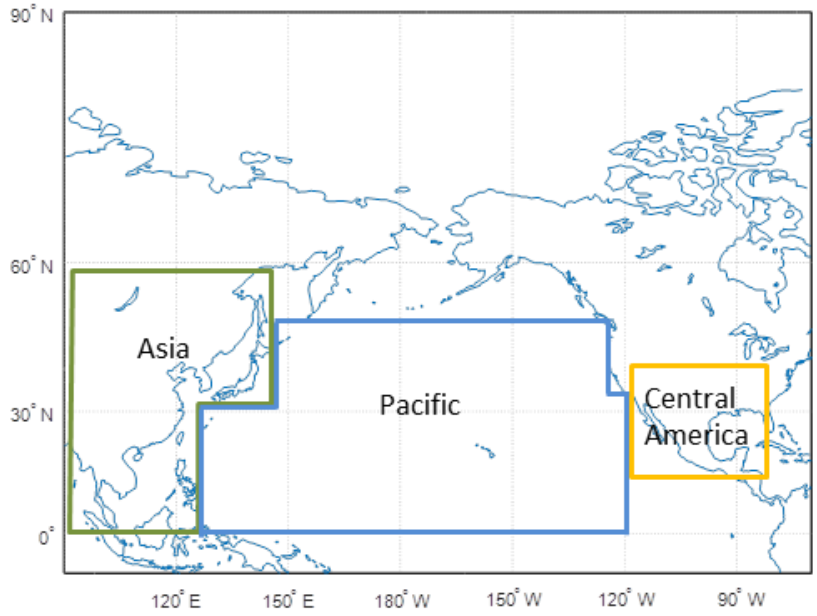

Figure 7. Geographical boundaries used to characterize the air parcels associated with the 12-day backward trajectories ending at TMF during the lidar measurements over the period 2000-2015

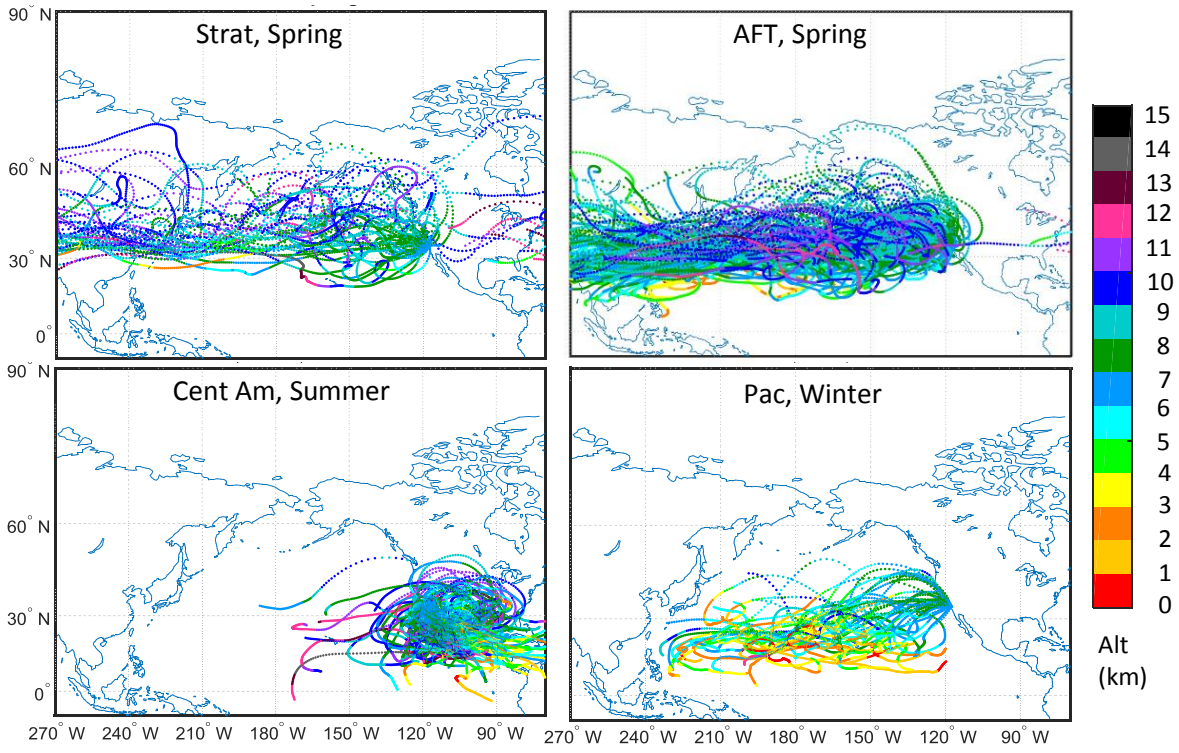

Figure 8. Examples of HYSPLIT 12-day backward trajectories arriving at TMF at 7 km altitude for four selected seasons and categories (see text for details)

Figure 9. Distribution of the five categories identified for each trajectory ending at TMF during the lidar measurements over the period 2000-2015. The number of occurrences is given in percentage for each month of the year, and for four different altitude layers

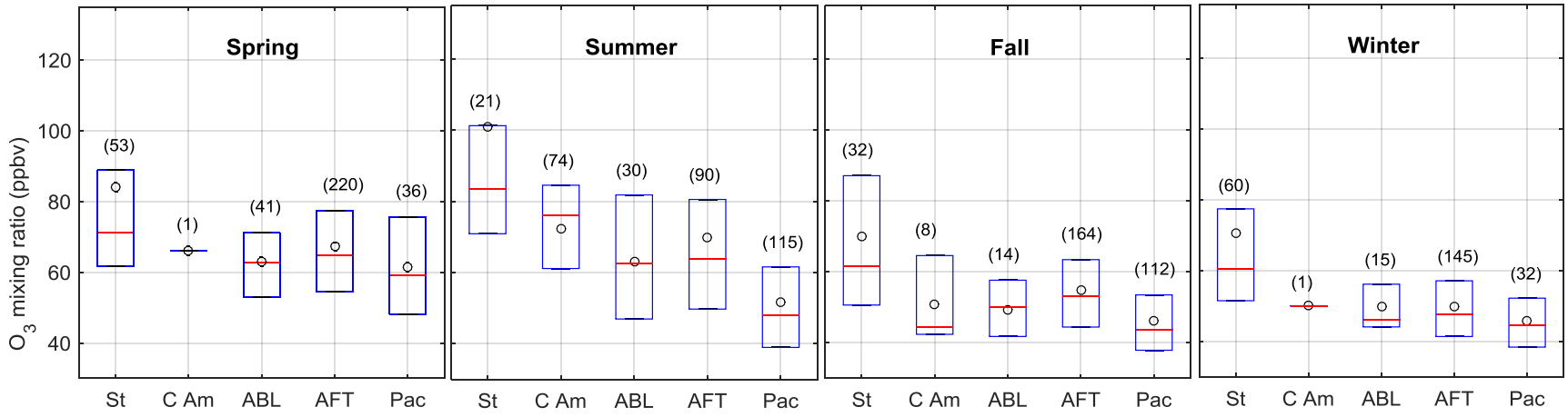

Figure 10. Box plot of the ozone mixing ratios measured within the air masses arriving at TMF at 9 km for the five identified categories (see text for details) and the four seasons. The black dot represents the mean value, the red line is the median and the box limits correspond to the 25th and 75th percentiles. The numbers between parentheses indicate the number of associated trajectories

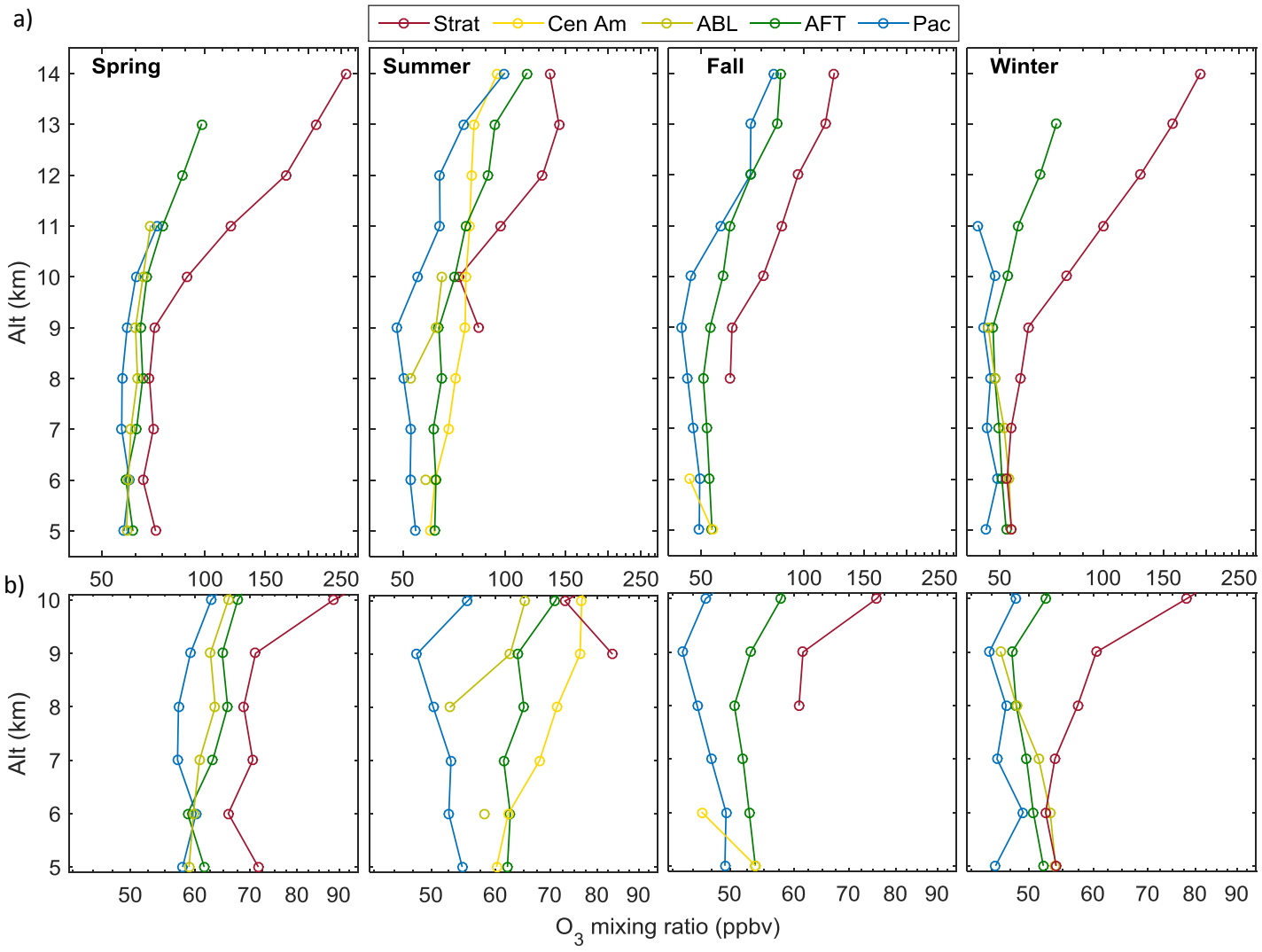

Figure 11. a) Composite profiles of the ozone mixing ratio associated with the different categories and for each season. Results are shown only when the number of samples for a given category was larger than 5% of the total number of samples in that season. b) Same as a) but zoomed in the region from 5 to 10 km.

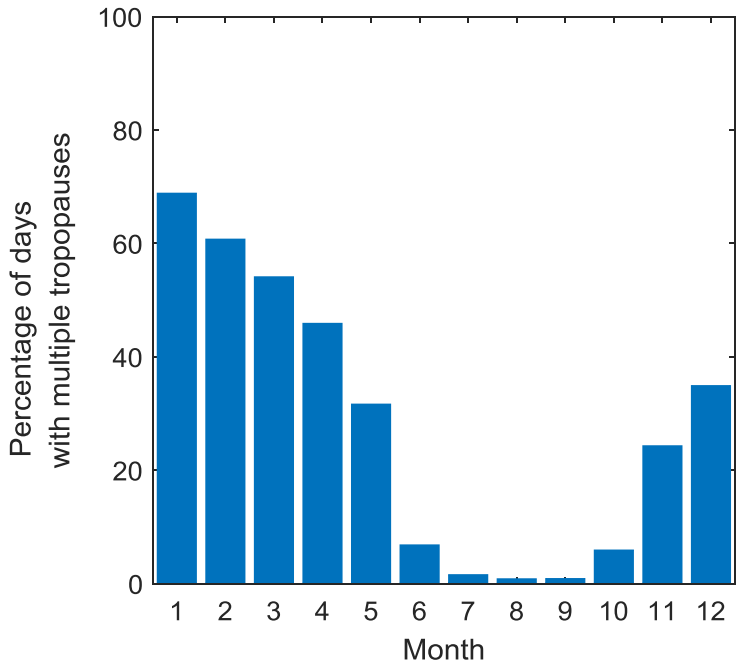

Figure 12. Monthly distribution of occurrences (in %) of double tropopauses above TMF. The number of days with tropopause folds is normalized to the total number of measurements per month compiled in Table1

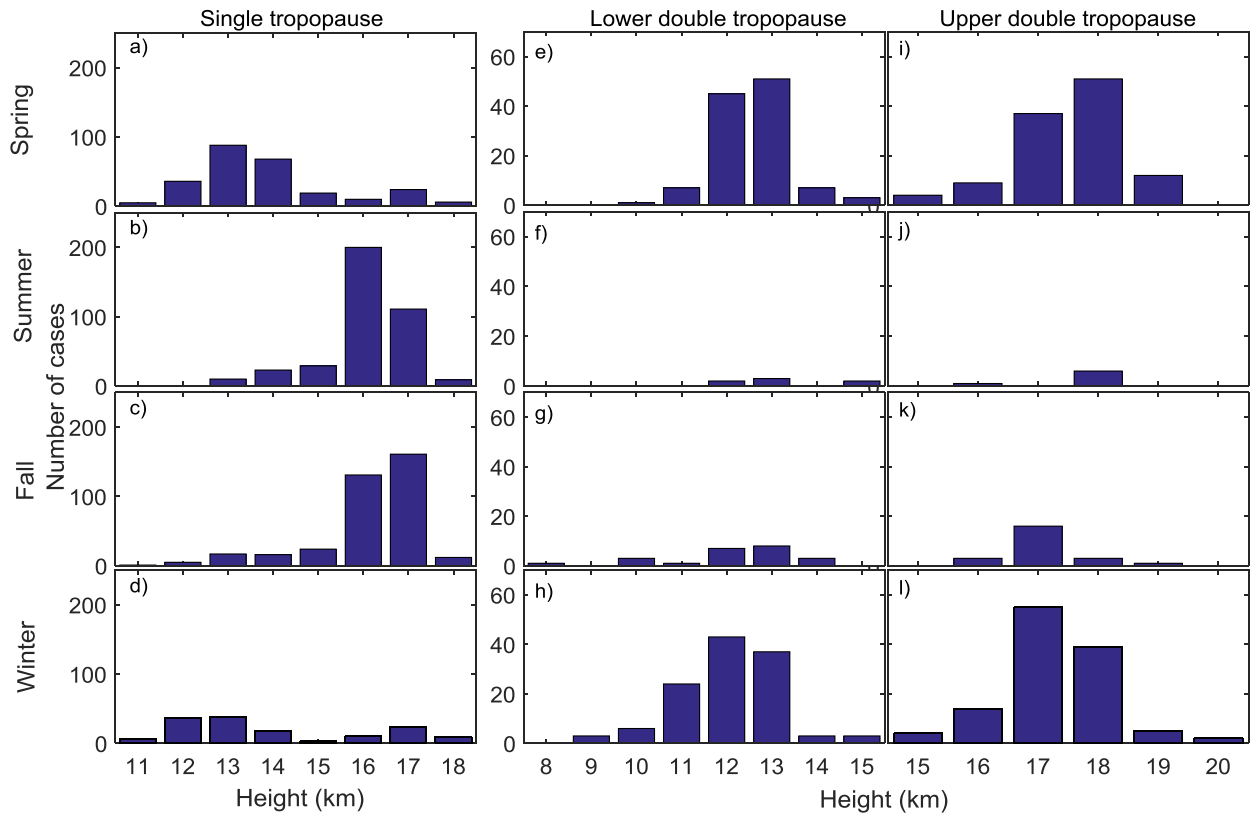

Figure 13. a) to d) Altitude distribution of the tropopause above TMF for spring, summer, fall and winter respectively, and in the absence of double-tropopause. e) to h) Altitude distribution of the lower (first) tropopause above TMF for spring, summer, fall and winter respectively, and in the presence of a double-tropopause. i) to l) Same as e) to h) but for the upper or second tropopause. All computations were made at the times of the TMF lidar measurements

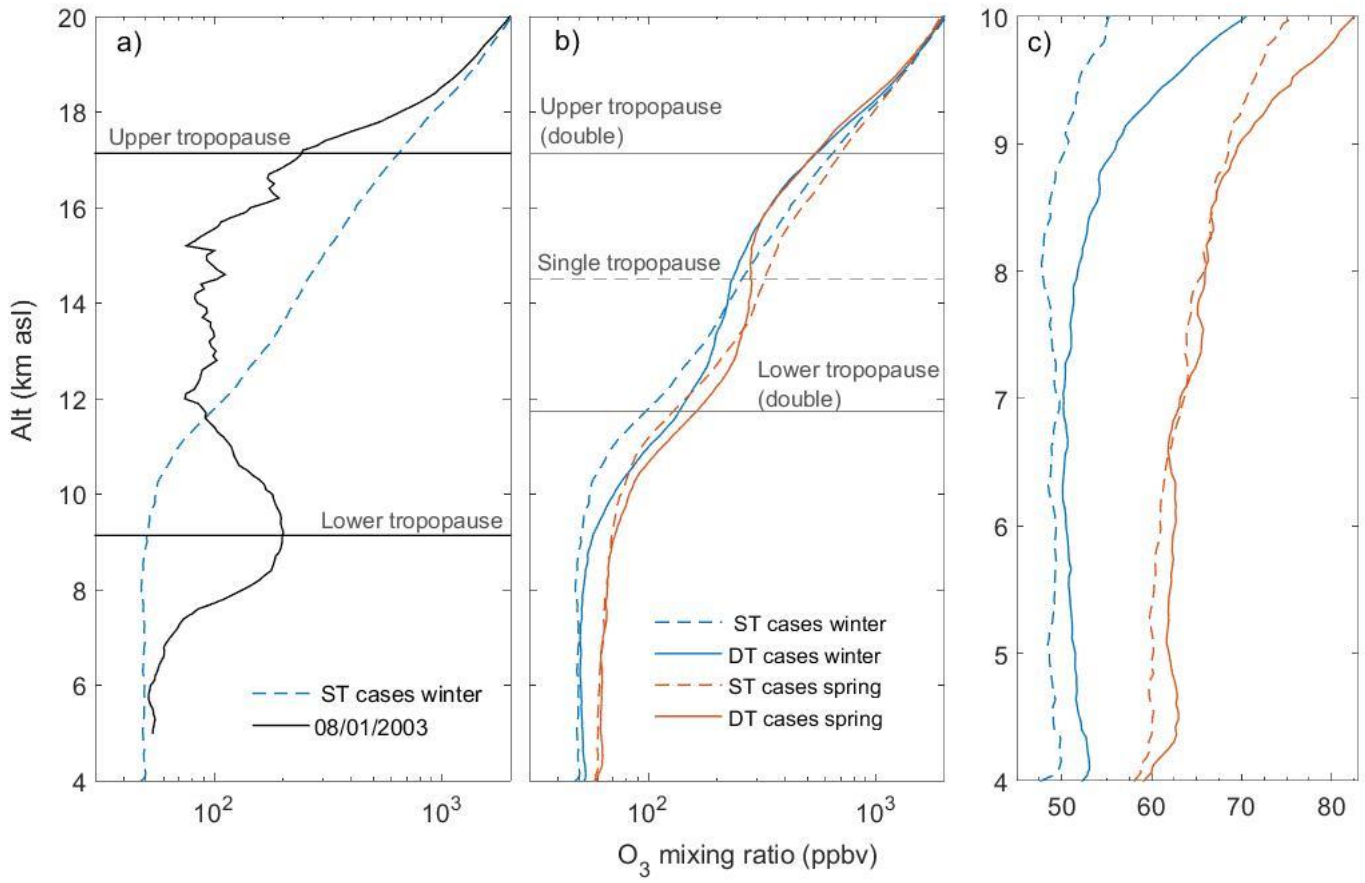

Figure 14. a)Ozone mixing ratio profile on January 8, 2003 (black line) and winter averaged ozone mixing ratio profile computed in the presence of single tropopause above TMF (blue dashed line). The horizontal solid black lines depict the altitude of the lower and upper tropopauses on June 8, 2013. b)Winter- (cyan) and Spring- (red) averaged ozone mixing ratio profiles computed in the presence of a double tropopause (DT, solid curves) and single tropopause (ST, dashed curves). The horizontal solid grey lines depict the average altitude of the lower and upper tropopauses when a double tropopause was identified. The horizontal dashed grey line corresponds to the average altitude of the tropopause when a single tropopause was identified. c) Same as b) but zoomed on the tropospheric part of the profiles (4-10 km)